

# Exchanges of Atmospheric CO<sub>2</sub> and <sup>13</sup>CO<sub>2</sub> with the Terrestrial Biosphere and Oceans from 1978 to 2000.

## III. Sensitivity Tests

Stephen C. Piper<sup>1</sup>, Charles D. Keeling<sup>1</sup>, and Elisabeth F. Stewart<sup>1</sup>

**Abstract**—Simulated sources and sinks of atmospheric CO<sub>2</sub>, calculated by a three-dimensional tracer inversion model of the global carbon cycle, have been subjected to tests to determine their sensitivity to uncertain model specifications and input data. The model, described in a companion article [Piper et al., 2001a], employs regional CO<sub>2</sub> source components as boundary conditions to a three-dimensional transport model, TM2, driven by observed winds and a vertical convection scheme based on both observational data and dynamic theory. The model, by an inverse calculation, adjusts the strengths of 7 source components, pertaining to boreal, temperate, and tropical zones, to achieve an optimum fit to measurements of atmospheric CO<sub>2</sub> concentration and <sup>13</sup>C/<sup>12</sup>C isotopic ratio from 1981 through 1999 at an array of 9 stations. A standard reference fit was made using initial choices of model parameters and input data for wind, convection, temperature, solar irradiance, remotely sensed plant activity, and related factors, expressed as averages over as many years of recent data as were available for each, but with respect to winds and convection just for the year 1986. This standard case is challenged by means of sensitivity tests in which model specifications and input data have been varied. Although temporal variability in simulated oceanic and terrestrial biospheric sources and sinks deduced in this standard case mainly reflects variability in observations of atmospheric CO<sub>2</sub>, as much as a fourth is found to be owing to variable wind and convection, and some is likely to be due to temporally varying errors in the specification of CO<sub>2</sub> emissions from fossil fuel which lead to nearly compensating departures in inferred biospheric fluxes. Averages of deduced fluxes and the patterns of variability are found to be only slightly sensitive to model specifications, except for the distribution of terrestrial fluxes near the La Jolla sampling site, set *a priori*, which strongly affects the deduced strength of the northern temperate biospheric sink. As a preferred model solution for further study of relationships to environmental factors and for comparison with other investigations, we adopted the specifications of the standard case in all respects except the distribution of sources and sinks in the vicinity of our observing station at La Jolla, California which is close to an urban area. Both the standard and preferred cases, supported by sensitivity tests, indicate that the terrestrial biosphere has been a sink of atmospheric CO<sub>2</sub> in the temperate latitudes of both hemispheres over the past two decades, a source in the tropics and boreal zone. The oceans have been sinks everywhere except in the tropics.

### PREFACE

This is the third of four articles that seeks to characterize sources and sinks of atmospheric carbon dioxide from direct measurements of the concentration and <sup>13</sup>C/<sup>12</sup>C ratio of atmospheric CO<sub>2</sub>. The articles, organized as though chapters of a single study, are referred to henceforth as Articles I to IV corresponding, respectively, to Keeling et al. [2001], Piper et al. [2001a,b], and Keeling and Piper [2001].

<sup>1</sup>Scripps Institution of Oceanography, University of California, San Diego, California

### 1. INTRODUCTION

The phenomena addressed in this study are too complex to allow identification of all possible errors that could call into question the findings described in Articles I and II. We strive, however, in so far as possible, to assess the reliability of these findings. In Article II, we addressed clearly recognizable sources of error, determinable by standard statistical methods. In the present paper, we address systematic errors, some of which are more serious, but less precisely determinable.

We rely largely on sensitivity tests to make evident which of our findings are likely to survive future scrutiny. Shortcomings in our analysis relate, in part, to inadequate or incomplete sets of critical ancillary environmental data, which may be remedied in the future. Thus, our analysis should be judged not solely on the basis of irrefutable findings, but, also on the potential for more definitive findings when better data become available.

In the tests described below, we make changes, usually one parameter at a time, to a standard reference calculation, henceforth, "standard case", described in detail in Article II. This calculation prescribes 11 source components representing sources and sinks of atmospheric CO<sub>2</sub>: 5 terrestrial biospheric, 5 oceanic, and 1 for fossil fuel emissions. Also 4 adjustable biospheric source components are used, distributed in proportion to spatially variable net primary production of plants (NPP) in zones, divided at 23.5°S and N and at 47°N, roughly matching the major climate zones: boreal, north and south temperate, and tropical. Similarly, 3 adjustable oceanic source components are used, distributed proportionally to a spatially variable air-sea CO<sub>2</sub> exchange coefficient, in zones divided at 23.5°N and S. The distribution of the tropical zone component is also made proportional to observations of the air-sea difference of pCO<sub>2</sub>. The atmospheric CO<sub>2</sub> response ("model solution") to each of these source components is computed by the TM2 atmospheric transport model of Heimann [1995], using analyzed winds for 1986 from the European Center for Medium Range Forecasts (ECMWF) regrided to a horizontal resolution of 8x10° and 9 vertical levels. The source solutions are then summed to produce a "composite model solution" representing the 3-dimensional distribution of atmospheric CO<sub>2</sub> concentration relative to a background concentration (see Article II, subsection A.1). Seasonal CO<sub>2</sub> variations are produced primarily by biospheric source components separately representing NPP and heterotrophic respiration (RES), which are parameterized simultaneously by a fit to seasonal observations of atmospheric CO<sub>2</sub> for 1986 at three northern atmospheric CO<sub>2</sub> observing stations. Smaller seasonal variations

are contributed by other source components, some prescribed to vary seasonally, and others prescribed to be nonseasonal but indirectly producing seasonal variations via interaction with seasonally-varying atmospheric transport (see Article II, Table 3). Model solutions are similarly calculated for the distribution of the  $^{13}\text{C}/^{12}\text{C}$  ratio of  $\text{CO}_2$ . The annual strengths of the adjustable source components are then determined at overlapping 6-month time-steps to produce optimal fits of the summed model responses of all source components to observations of both atmospheric  $\text{CO}_2$  concentration and  $^{13}\text{C}/^{12}\text{C}$  isotopic ratio at our  $\text{CO}_2$  observing stations, and to sum to global constraints calculated by a double deconvolution procedure, described in Article I.

The sensitivity tests, described below, challenge major aspects of the standard case: portrayal of atmospheric transport, method of inverse calculation, configuration of the source components and our observational network, evolution of the fossil fuel  $\text{CO}_2$  source, and specification of isotopic processes. Additional tests, described by Keeling et al. [1989, pp. 337-350], also provide insight regarding our choice of parameters. It will be shown that the tests almost all support, as optimal, the choices of procedures and model parameters of the standard case. An exception is with respect to the distribution of sources and sinks close to the observing station at La Jolla, California. To arrive at a preferred case, as explained in subsection 5.3, below, we modify the standard case by removing the land-based sources and sinks from the grid box in which La Jolla is situated.

## 2. SENSITIVITY TO ATMOSPHERIC TRANSPORT

### 2.1 Replacement of 1986 data by 1987 data

In our presentation of sensitivity tests, beginning with this subsection, we show plots of zonal oceanic and terrestrial biospheric fluxes, similar to the format of Article II, Figure 4. Since these fluxes tend to show a relation to large scale weather events related to the El Niño phenomenon (see Article I), we again indicate the approximate timing of these events in each plot by gray bars.

In this first test, we substitute 1987 meteorological fields for the 1986 fields of the standard case (see Article II, Figure 4) to assess the effect of interannual variations of atmospheric transport for the single additional year for which we have complete data sets for wind and convection for the TM2 atmospheric transport model. The effect of this substitution, for all years of simulation (Figure 1), is to produce almost constant shifts in fluxes from those of the standard case, also plotted in Figure 1. The main impact of changing wind fields is on the strengths of the zonal average terrestrial biospheric fluxes, up to  $\pm 0.9 \text{ PgC yr}^{-1}$ , the oceanic fluxes changing by less than  $0.15 \text{ PgC yr}^{-1}$  everywhere except in the tropics. We further determined (results not shown) that the main impact of the change in meteorological fields is on the strength of the seasonal biospheric source components, NPP and RES.

We tested the relative importance of winds versus convection by separately swapping them in simulations in which all source components were set to the same strengths as in the standard calculation. The atmospheric  $\text{CO}_2$  responses,

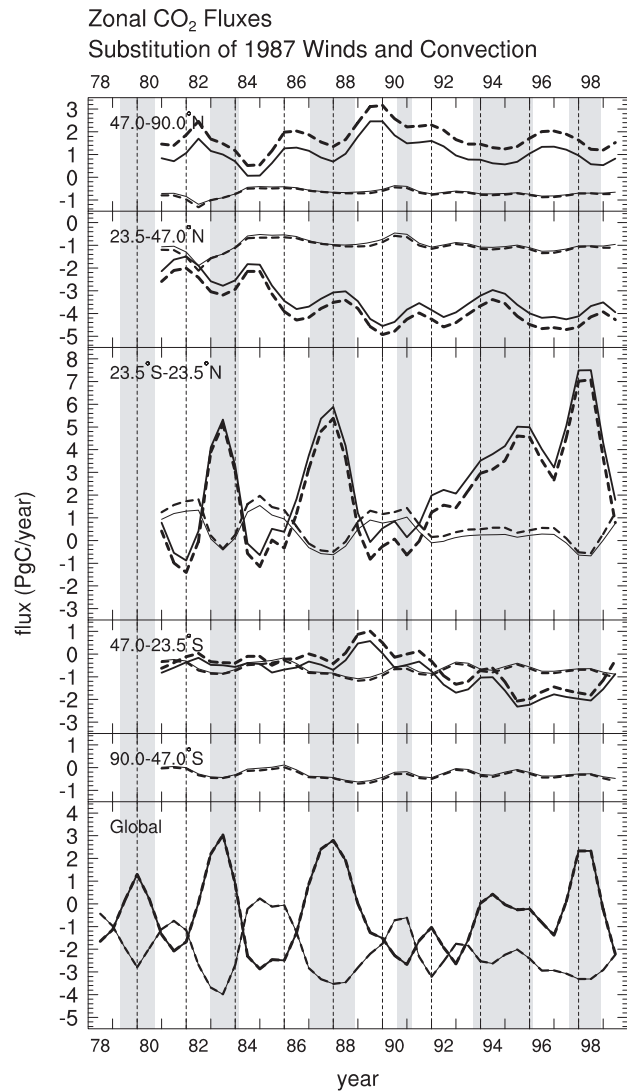


Fig. 1. Net annual  $\text{CO}_2$  exchange fluxes, representing exchanges of atmospheric  $\text{CO}_2$  with the oceans (thinner lines) and terrestrial biosphere (thicker lines), in  $\text{PgC yr}^{-1}$ , determined by an inversion calculation for geographic zones as labeled in 5 panels. A 6th, bottom, panel shows global sums of these fluxes determined by a deconvolution procedure. In all panels, solid lines show fluxes determined by a standard reference calculation ("standard case"); dashed lines show fluxes determined by an alternative calculation in which wind and convection fields for 1987 are substituted for 1986 fields, as a test of the sensitivity of the calculations to the choice of meteorological data. Gray bars demarcate approximately the times of El Niño events, inferred from time-intervals during which the rate of change of atmospheric  $\text{CO}_2$  concentration at Mauna Loa Observatory, Hawaii, exceeded the trend in industrial  $\text{CO}_2$  emissions, as shown in Article I, Figure 5.

relative to the standard case, are shown as a function of latitude in Figure 2. Zonal fluxes inferred for two of the four combinations of 1986 and 1987 winds and convection are listed in Table 1. This test shows that concentration differences from the standard case produced at the northernmost stations, Alert and Point Barrow, are owing almost entirely to swapping winds, whereas, farther south, swapping convection has a substantial effect. However, there is not a simple monotonic relationship with latitude. For example, at  $40^\circ\text{N}$ ,  $145^\circ\text{W}$  in the north Pacific Ocean (formerly Weather Station P), swapping 1987 for 1986 convection has less effect than at  $63^\circ\text{N}$ , in

southern Alaska. Convection appears to be a more important factor than winds in predicting interannual changes in our observations for La Jolla and stations farther south, but the changes are generally small. Thus a test described in the next subsection, varying the winds but not convection, tests the major influence of interannually-varying atmospheric transport on our inverse calculations.

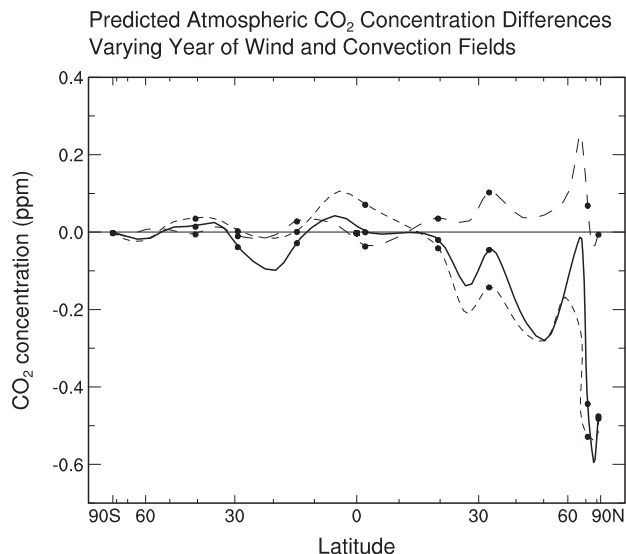


Fig. 2. North-south profiles of the departures of mean annual  $\text{CO}_2$  concentration, in ppm, from the standard case, predicted by substitution of 1987 fields for 1986 fields in three combinations: 1987 winds (short-dashed lines), 1987 convection (long-dashed lines), 1987 winds and convection (solid line). The lines are Akima spline curves connecting predictions for observing stations and intermediate points, as a visual aid. Solid circles show predictions for  $\text{CO}_2$  observing stations.

## 2.2 Influence of interannually-varying winds

To estimate the importance of using correct wind data for successive years in place of 1986 winds for all years, we carried out a model simulation with a set of meteorological fields produced by the ECMWF reanalysis project [Gibson et al., 1997]. The air mass fluxes of this reanalysis had been processed from 1979 through 1993 for use with a newer transport model, TM3, having hybrid rather than sigma model levels (see Article II, section 3). We were not able to implement daily convection fields for TM3, instead substituting monthly-averaged fields derived from the daily operational convection fields for 1986 for all years of simulation.

A multi-year simulation by direct inversion of atmospheric  $\text{CO}_2$  data fields was beyond the scope of our study. Instead, we made a forward multi-year simulation to establish the effect of interannually varying winds on the predicted distributions of  $\text{CO}_2$  concentration and  $^{13}\text{C}/^{12}\text{C}$  ratio. Fluxes of  $\text{CO}_2$  were then determined that were consistent with these altered distributions.

As input to the forward calculation, we used sums of the source components for atmospheric  $\text{CO}_2$  concentration and  $^{13}\text{C}/^{12}\text{C}$  ratio ("composite source fluxes" defined in Article II, subsection A.1, equation (A.2)) of the standard case, thus avoiding a need for multi-year runs for each of a large number

of source components. The composite sources of concentration and  $^{13}\text{C}/^{12}\text{C}$  were produced from July, 1980 through December, 1993 by adding the model source components with average strengths prescribed for every 6 months, as found for the standard case. Monthly time-steps for the sensitivity test were then obtained by linear interpolation. We initialized the multi-year simulation by cycling 3 times over reanalysis winds for 1979 and then once with winds for 1980. The simulation proceeded further with reanalysis winds and composite source fluxes matched in time to the end of the wind record. Then, for each of our  $\text{CO}_2$  observing stations, we compared the results with a second multi-year simulation that used only 1986 reanalysis winds. We thus established the effect of interannually varying wind fields on  $\text{CO}_2$  concentration where we had observations.

The most striking differences in calculated  $\text{CO}_2$  concentration, with interannual varying winds replacing winds just for 1986, are in the arctic, as shown for Alert station, at  $83^\circ\text{N}$  (Figure 3), where, as illustrated in Figure 2, replacing 1986 wind fields with those of 1987 produced large differences in predicted concentration for some years of the simulations. The differences are relatively small before 1986, a year in which the average difference is zero. For 1987, however, there is a sharp decline of 0.3 ppm, and then in 1988 a very sharp rise of 0.6 ppm, followed in 1992 and 1993 by a fall of 0.3 ppm. The latter two events are almost coincident with a rise in  $\text{CO}_2$  concentration at Alert and Point Barrow, Alaska, of the order of 2 ppm, independent of the long-term trend, followed by a fall of nearly the same magnitude (see Article I, Figure 2). Evidently, about a fourth of the unusually high  $\text{CO}_2$  concentrations observed at high latitudes from 1989 through 1992 can be attributed to interannual variations in transport by the winds.

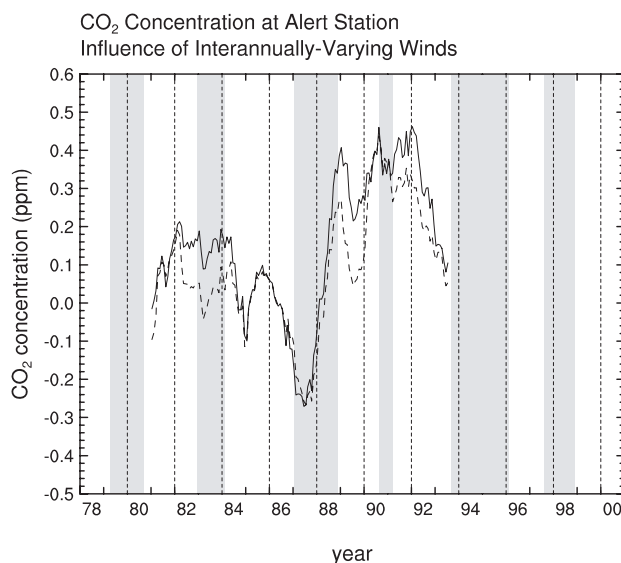


Fig. 3. Departures of predicted atmospheric  $\text{CO}_2$  concentration from the standard case in ppm, at Alert Station ( $82.5^\circ\text{N}$ ,  $62.3^\circ\text{W}$ ) with interannually-varying winds substituted for 1986 winds. A solid line shows concentration differences using all model source components in the prediction; a dashed line using only the components for net primary production (NPP) and heterotrophic respiration of land plants (RES). The curves have been smoothed by a 12-month moving average. Gray bars are as in Figure 1.

TABLE 1

COMPARISON OF ZONAL FLUXES, IN PG C PER YEAR, FROM INVERSE FITS TO 1987 ATMOSPHERIC CO<sub>2</sub> AND <sup>13</sup>C/<sup>12</sup>C OBSERVATIONS USING 1986 WINDS VERSUS 1987 WINDS

Year of Winds	Composite Flux <sup>a</sup>	90°-47°S	47°-23.5°S	23.5°S-23.5°N	23°S-47°N	47°-90°N	Global <sup>b</sup>
1986	bio	–	-0.46	+5.37	-3.35	+0.87	+2.42
1987	bio	–	-0.16	+4.81	-3.78	+1.55	+2.42
Difference			+0.31	-0.56	-0.43	+0.68	0
1986	oce	-0.41	-0.81	-0.58	-0.90	-0.63	-3.32
1987	oce	-0.44	-0.85	-0.44	-0.93	-0.64	-3.32
Difference		-0.04	-0.05	0.14	-0.03	-0.02	0

<sup>a</sup> "bio" denotes the composite terrestrial biospheric flux; "oce" the composite oceanic flux. Both are expressed positive into the atmosphere.

<sup>b</sup> The global fluxes, prescribed to match the predictions of the global deconvolution, are invariant.

We performed an additional multi-year simulation (dashed line in Figure 3) based solely on the seasonal biospheric source components, NPP and RES. The trend in difference for Alert station is nearly the same as that for the full model solution, supporting a finding from our comparisons for 1986 versus 1987 (not shown), that changing wind fields mainly affect atmospheric responses to the seasonal biospheric fluxes.

To approximate an inverse calculation with multi-year wind fields, we adjusted our atmospheric observations to reflect differences in both concentration and <sup>13</sup>C/<sup>12</sup>C ratios and performed an inverse calculation, as in the standard case, with the results shown in Figure 4. The primary effect of using interannual varying winds in place of 1986 winds is to reduce by as much as 0.5 PgC yr<sup>-1</sup> the terrestrial biospheric source flux of the boreal zone while increasing the corresponding northern temperate flux between 1988 and 1992, i.e., just during those years when a large increase was observed in atmospheric CO<sub>2</sub> concentration in the far north (Article I, Figure 2). Almost no changes are observed in the fluxes simulated for the tropical zone. Our calculations comparing the results of swapping operational winds and convection for 1986 and 1987 indicate, however, as shown in Figure 2 and Table 1, that the biospheric fluxes deduced in the tropics and southern temperate zone are affected by interannually-varying convection. The extent of this effect could not be determined, since we lack interannually-varying convection fields.

### 2.3 Change to 1998 winds and TM3 model

As an additional test of the influence of interannual variations in atmospheric transport, we performed a simulation with operational winds and convection for 1998. The 1998 fields are based on meteorological data processed by the analysis and forecasting system of ECMWF, as are the 1986 fields of our standard calculation. This system, however, underwent several modifications between 1986 and 1998 and therefore the comparison is not entirely consistent [ECMWF, 1999]. Also, the 1998 fields are inputs to the atmospheric transport model, TM3, rather than TM2 of the standard case. Owing to TM3 having a revised convection scheme and slightly different vertical levels, differences from the standard case obtained in this test are not caused solely by prescribed differences in

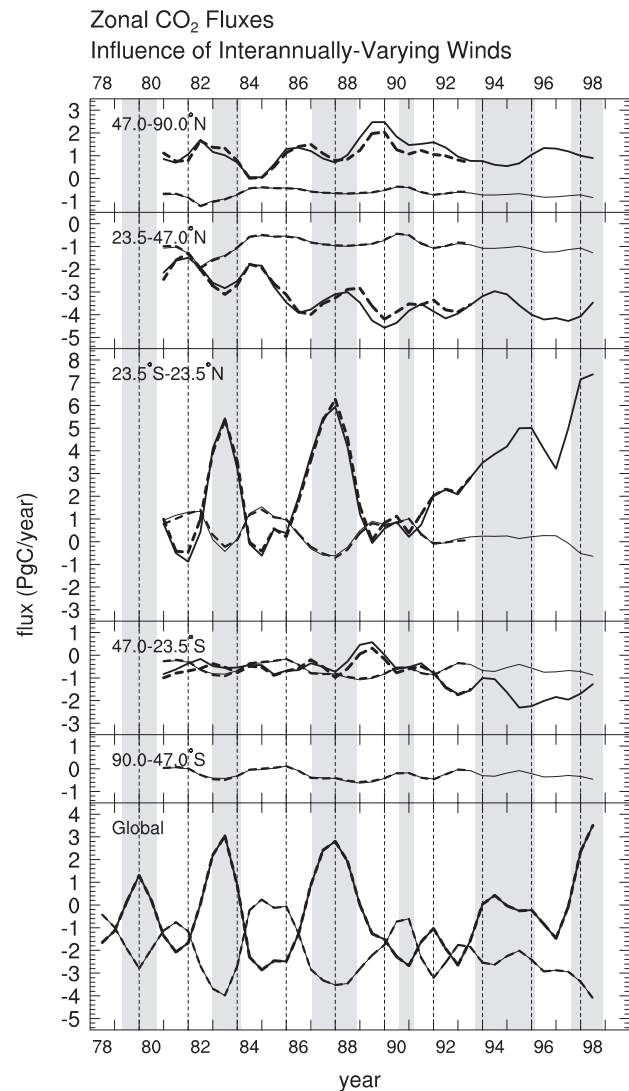


Fig. 4. Zonal fluxes, as in Figure 1, except that, for the sensitivity test, the fluxes are computed using interannually-varying winds from mid-1980 to the end of 1993, as in Figure 3. Vertical convection is interannually invariant, as described in the text.

wind fields. The resulting fluxes (Figure 5) have the same general features as for the standard case, but the tropical biospheric source is increased, offsetting decreases in the boreal and southern temperate zone fluxes. Even though the same winds are used for all years, in both the test simulation and the standard case, the tropical peaks during the El Niño events of 1983, 1987, 1994, and 1998 increase relative to the standard case more than the troughs, thereby increasing the interannual variability of the inferred tropical biospheric flux. This presumably relates in large part to the difference in convection fields, as suggested by the comparison of 1986 and 1987 winds described earlier.

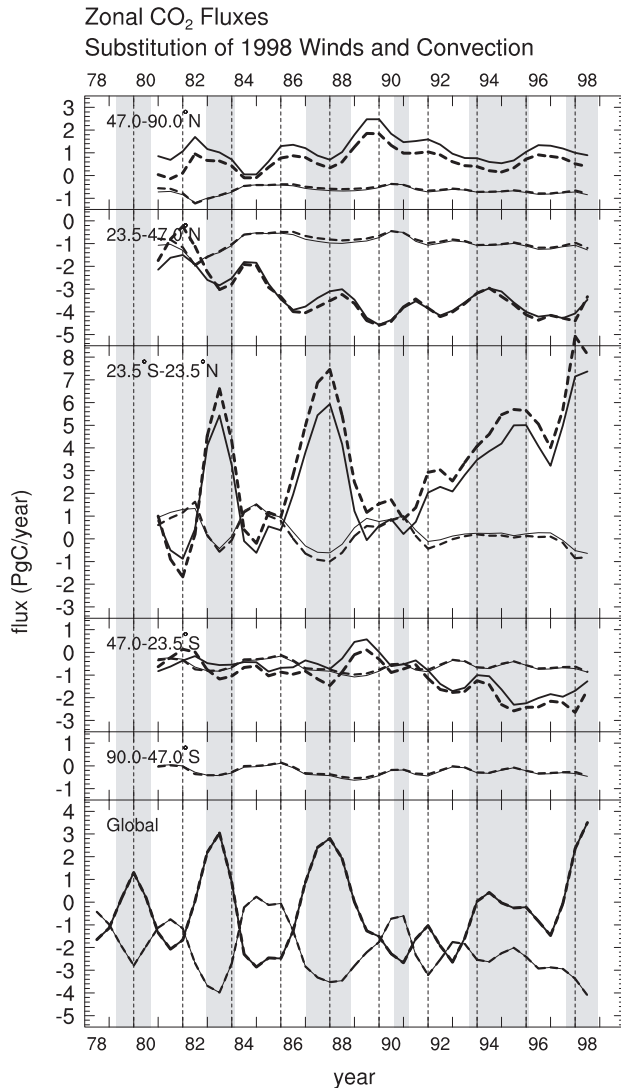


Fig. 5. Zonal fluxes, as in Figure 1, except that, for the sensitivity test, the TM3 transport model is used with 1998 winds and convection in the place of the TM2 model with 1986 winds and convection.

#### 2.4 Model comparison for vertical variation in polar seasonal cycle

Neither transport model, TM2 or TM3, defines an explicit planetary boundary layer (PBL) that simulates such small scale features as a nocturnal temperature inversion restricting

vertical mixing of the air column at night. The lowest layers of TM2 and TM3, with their tops at geopotential heights of 0.44 km and 0.48 km, respectively (cf. last column of Table 2, Article II) do not reflect the PBL when it is lower than these tops, for example during conditions of temperature inversion near the ground. Because the air tends to mix vertically to a height greater than the lowest layers of these models, at least briefly almost every day when there is metabolic activity of plants and soil causing locally varying  $\text{CO}_2$  concentration, we have assumed that an explicit PBL is not needed to establish the mean annual concentration of atmospheric  $\text{CO}_2$  in this study. It has been suggested, however [Denning et al., 1995], that the PBL confines  $\text{CO}_2$  from plant metabolism to a greater extent near the ground than models like TM2 and TM3 predict, with the consequence that these models underestimate the biospheric sink for atmospheric  $\text{CO}_2$  at higher latitudes where the PBL is most strongly developed.

As a test of how well TM2 and TM3 simulate the vertical transport of atmospheric  $\text{CO}_2$ , we have compared their ability to predict the attenuation of the seasonal cycle of  $\text{CO}_2$  in the Arctic near Point Barrow, Alaska, using the same source components as for the standard case (Figure 6). It is evident that TM3 more strongly attenuates the seasonal signal of  $\text{CO}_2$  than TM2. Also plotted in Figure 6 is an estimate of the actual attenuation in the Arctic, based on air samples collected in the late 1950's by aircraft flying at 700 and 500 hPa pressure heights between the coast of Alaska and the North Pole, and on ground-level air collected in the early 1960's near the aircraft transect line, at Point Barrow, Alaska. Data for Mauna Loa Observatory, Hawaii [Keeling et al., 1996] indicate that the amplitude of the seasonal cycle in the northern hemisphere varied by only a few percent over this span of years, although it has varied more since (data not shown). The observed attenuation is somewhat greater than predicted by the TM2 simulation, mainly seen at the 700 hPa level; it is substantially less than predicted by the TM3 simulation, thus lending no support for a stronger PBL than that model provides. We note, furthermore, that our study does not require a prediction of the average concentration of atmospheric  $\text{CO}_2$  close to the ground in substantially vegetated regions where the daily average concentration at sampling height may be substantially higher than above the PBL because  $\text{CO}_2$  from respiration accumulates in a stagnant inversion layer at night raising the daily average to higher concentrations near the ground than aloft. We strive to have air sampled only where diurnal variability is negligible or selectively, when the air is vertically well mixed.

### 3. SENSITIVITY TO THE METHOD OF INVERSE CALCULATION

For the standard case, we adopted a "quasi-stationary" mode of computation in which the interannual time-history of sources and sinks on  $\text{CO}_2$  concentration is ignored, continuing the simplified computation of  $\text{CO}_2$  transport introduced by Heimann and Keeling [1989]. We have assumed, in essence, that the ultimate global redistribution of atmospheric  $\text{CO}_2$  arising from a pulse of  $\text{CO}_2$ , added or removed from the

TABLE 2  
REDUCED CHI-SQUARE STATISTICS FOR SENSITIVITY TESTS

Sensitivity Test	Reference to:	Averaging Period		
		1986-1989	1990-1998	1986-1998
Standard case	All figures cited	5.28	4.28	4.59
Substitution of 1987 winds	Figure 1	6.55	5.08	5.53
Substitution of 1998 winds	Figure 5	7.39	6.16	6.54
Biospheric boundaries shifted to 16°	Figure 8	4.86	3.87	4.17
Biospheric boundary shifted to 55°N	Figure 9	4.84	4.33	4.48
Biospheric buffer zones set to zero	Figure 10	5.15	4.14	4.45
New oceanic boundary at 47°N	Figure 11	5.68	4.32	4.74
New oceanic boundary at 47°S	Figure 12	5.59	4.02	4.50
Christmas Island data excluded	Figure 13	5.10	4.10	4.41
Data restricted to complete records	Figure 14	6.90	3.16	4.31
Terrestrial sources near La Jolla set to zero	Figure 15a	6.15	4.80	5.22
Also terrestrial sources east of La Jolla	Figure 15b	6.22	5.08	5.41
Also La Jolla location shifted	Figure 16	5.38	4.40	4.70
<sup>13</sup> C/ <sup>12</sup> C data ignored	Figure 17	4.39	3.76	3.95
Industrial CO <sub>2</sub> source varied	Figure 19	5.23	4.11	4.45
C4 plant discrimination ignored	Figure 20	4.99	3.88	4.22
No oceanic temperature-dependent fractionation	Figure 22	15.55	10.44	12.01
Northern temperate terrestrial sink set to zero	–	13.77	15.31	14.83

TABLE 3  
NET TERRESTRIAL BIOSPHERIC CO<sub>2</sub> FLUXES COMPARED WITH NPP FOR 5 LATITUDINAL ZONES<sup>a</sup>

	Standard Case		Preferred Case		NPP <sup>b</sup>
	PgC yr <sup>-1</sup>	% of NPP	PgC yr <sup>-1</sup>	% of NPP	PgC yr <sup>-1</sup>
47-90°N	+1.08	(9)	-0.11	(-1)	11.6
23.5-47°N	-3.83	(-33)	-2.09	(-18)	11.7
23.5S-23.5°N	+3.38	(10)	+2.60	(8)	32.8
23.5-47°S	-1.40	(-27)	-1.17	(-23)	5.2
47-90°S <sup>c</sup>	-0.01	(-27)	-0.01	(-23)	0.1
Global	-0.79	–	-0.79	–	61.3

<sup>a</sup> Fluxes to the atmosphere averaged for 1990-1999 are positive numbers.

<sup>b</sup> Averaged from 1982-1990 (see Article II, subsection A.10)

<sup>c</sup> Terrestrial biospheric flux set to have same ratio to NPP as for the 23.5–47°S zone.

atmosphere locally, can be represented by an atmospheric response found by repeating the pulse over four years. We deem this assumption to be a reasonable approximation because the exchange time for north-south interhemispheric exchange, the longest mixing time for the atmosphere as a whole, is the order of one year [Jacob et al., 1987; Denning et al., 1999], and the interannual variations of sources are relatively small.

To test this quasi-stationary assumption, where “quasi” allows for seasonal and shorter-term temporal variability, we have carried out an alternative “extended response” mode of computation in which the redistribution is represented by a time-dependent series of four annual atmospheric distributions produced by a single CO<sub>2</sub> pulse in the first year, as described in Article II (Appendix B, section B.2). For this test, as explained in Appendix B of Article II, we use a simplified but functionally similar set of source components to those of the standard case. Calculations were made only at 12-month intervals.

Zonal fluxes computed in this extended response mode at

yearly intervals show greater interannual variability than the standard case, but usually by less than  $\pm 0.2$  PgC yr<sup>-1</sup> (Figure 7), differing most in the tropical zone near times of extreme peaks and troughs. We conclude that the errors introduced by the quasi-stationary calculation are generally too small to warrant use of this more complex mode of computation until a still more realistic continuous mode of computation is made possible by the availability of multi-year wind and convection fields for all years of simulations.

#### 4. SENSITIVITY TO THE CONFIGURATION OF SOURCE COMPONENTS

##### 4.1 Source component boundaries shifted

Our choices of boundaries for inverse calculations are challenged by sensitivity tests in which these boundaries are moved by one latitudinal grid width of 180°/23 from the standard case. It is sufficient to show two examples, both involving the terrestrial source components: the tropical zone

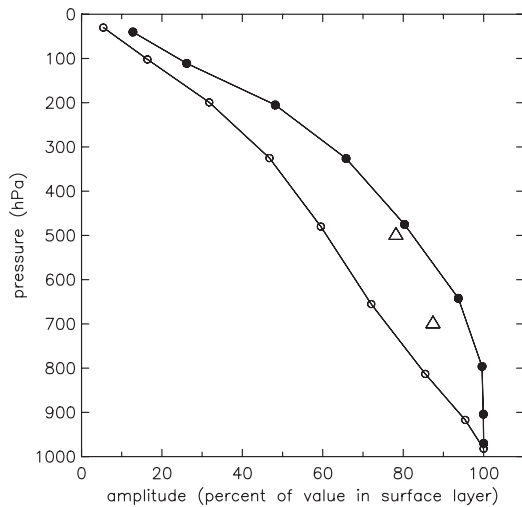
Seasonal Amplitude of CO<sub>2</sub> Concentration Versus Pressure Level

Fig. 6. Vertical variation in the relative amplitude of the seasonal cycle of atmospheric CO<sub>2</sub> (triangles) adjusted to a datum of 1 January, 1960, from samples of air collected by aircraft between 71.3° and 86.0° N, over the Arctic ocean [Keeling et al., 1968, Table 3; see also Bolin and Keeling, 1963, Figure 28]. The vertical scale is expressed by pressure levels in hPa. The amplitudes, for 700 and 500 hPa, were determined from 4-harmonic fits to monthly data and are compared with predictions using transport models TM2 (solid circles) and TM3 (open circles). Amplitudes for observations are relative to the amplitude at ground level from Jan., 1962 through Sept., 1963, for Point Barrow, Alaska (71° N.), a station close to the aircraft flight paths [cf. Keeling and Whorf, 1996, Figure 2b]. Model predictions are averages for both end points of the aircraft sample tracks, calculated at 9 model levels, and also expressed by 4-harmonic fits relative to Point Barrow. The wind data for TM2 are for 1986, those for TM3 are for 1998.

shrunk from 23.5° to 15.6° in each hemisphere, and the temperate-boreal boundary shifted northward from 47.0° to 54.8°N. In Figures 8 and 9, respectively, we show the results of these shifts, still plotted for the original zones of the standard case. Owing to alternating sources and sinks between tropical, temperate, and boreal in the standard case, a direct, trivial effect of boundary shifting is to force the covarying fluxes of individual grid boxes within the model zones into broader or narrower zones, thereby directly causing average flux magnitudes within the original zones to change. To a lesser extent there are additional adjustments stemming from altered north-south gradients which force a readjustment of the fit to CO<sub>2</sub> observations. The oceanic fluxes, as expected, are negligibly altered.

The overall effect of a tropical boundary shift is merely to cause a small transfer of the tropical biospheric source to the adjacent temperate zones. This result is not surprising because net primary production (NPP), maximal near the equator, falls off sharply poleward of 16°, especially in the northern hemisphere (see Article II, Figure 1). Therefore, because our model spatially prorates biospheric fluxes to NPP, only relatively small shifts in flux are involved when the tropical boundaries are shifted.

Shifting the temperate/boreal boundary causes more substantial changes. If the only changes taking place in zonal net fluxes were in apportioning between zones, the average flux poleward of 47.0°N. would change from a source of 1.1 PgC

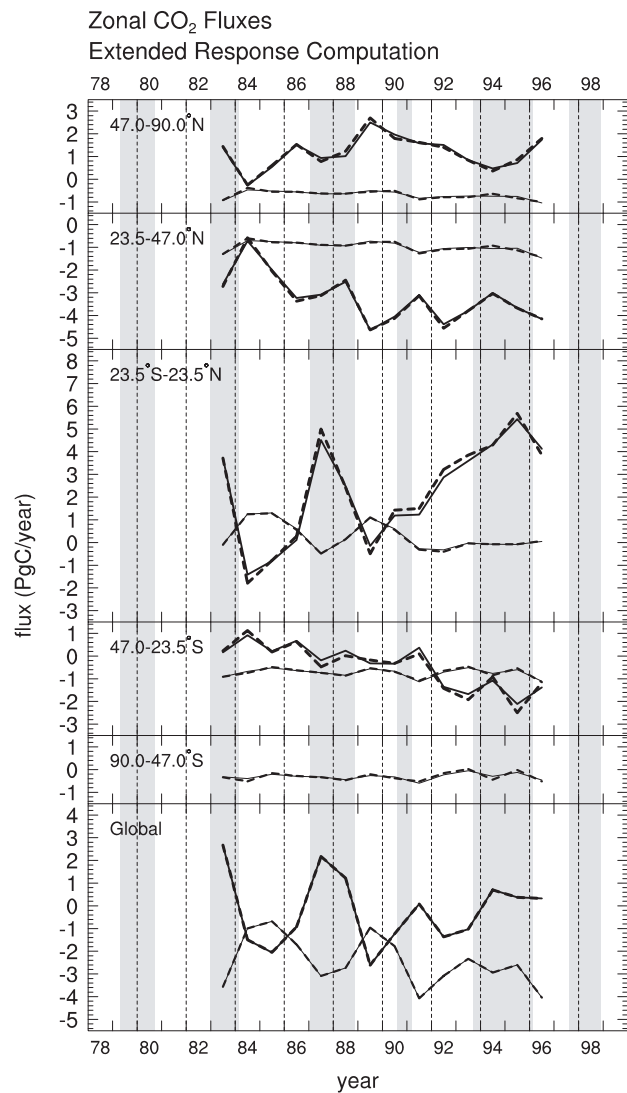


Fig. 7. Zonal fluxes, as in Figure 1, except that, for the sensitivity test, as described in the text, an extended response mode of computation (dashed lines) is implemented in place of a quasi-stationary mode of calculation (solid lines), similar to, but an earlier version of, the inversion model used for the standard case of this study.

yr<sup>-1</sup> to a sink of -0.1 PgC yr<sup>-1</sup>. This follows because the distribution of NPP, which is used to apportion the biospheric fluxes, changes with the shift in boundary from 11.6 (cf. Article I, Table 5) to 6.1 PgC yr<sup>-1</sup> in the boreal zone, and from 11.8 to 17.3 PgC yr<sup>-1</sup> in the northern temperate zone. The fit value for the boreal source, however, is +0.2 PgC yr<sup>-1</sup>, indicating only a small actual increase. Similarly, the fit value for the sink between 23.5° and 47.0°N. is actually increased from the standard case only by 0.4 PgC yr<sup>-1</sup>. Fluxes in the tropical and southern temperate zones are slightly altered. Thus, shifting boundaries by one grid spacing has little effect on the actual strengths of inferred fluxes. Also, as the plots indicate, the interannual variability in fluxes is negligibly affected.

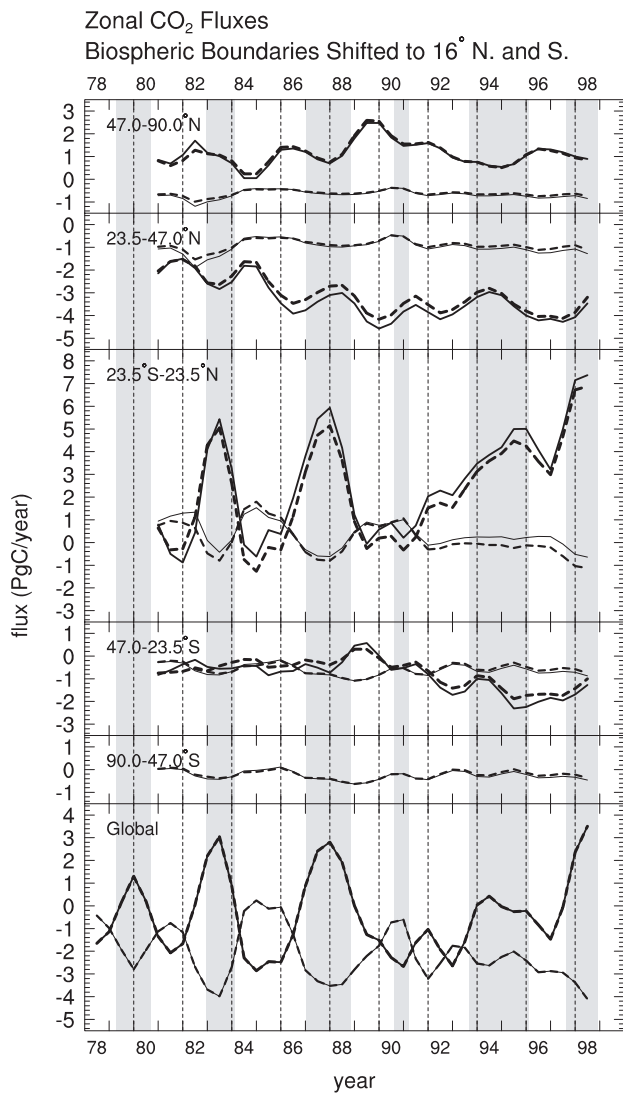


Fig. 8. Zonal fluxes, as in Figure 1, except that, for the sensitivity test, zonal boundaries at  $23.5^\circ$  in both hemispheres are shifted to  $15.6^\circ$ . Because, in the standard case, the adjustable tropical oceanic source component is zero between  $15.6^\circ$  and  $23.5^\circ$  in each hemisphere, shifting these boundaries affects only the adjustable biospheric components.

#### 4.2 Introduction of zero flux buffer zones

Stable inversion calculations in our model, achieved by defining broad zones, has led to abrupt transitions between inferred sources and sinks at some boundaries, as discussed above. A means to reduce this abruptness is to interpose a buffer zone close to such a boundary. We have examined this option in a sensitivity test that establishes buffer zones between  $47.0^\circ$  and  $54.8^\circ\text{N}$ ., and between  $15.6^\circ$  and  $23.5^\circ$  in both hemispheres, within which the terrestrial biospheric flux is set to zero. The effect of adding the northernmost buffer zone is to shrink the boreal zone without affecting the domain of the adjacent temperate zone. Both the boreal source and the northern temperate sink are reduced by about  $0.4 \text{ PgC yr}^{-1}$  (Figure 10), because the north-south gradient in  $\text{CO}_2$  concentration that the model seeks to predict is achieved with a lesser boreal flux when confined to a more northerly average location. Since such abrupt transitions between zones are likely

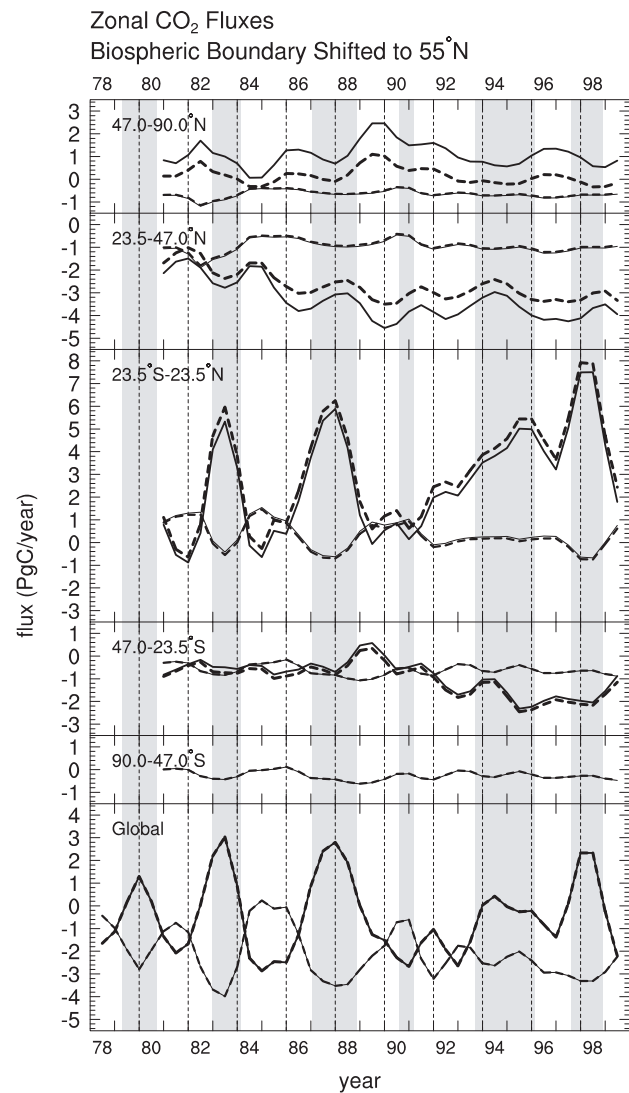


Fig. 9. Zonal fluxes, as in Figure 8, except that, for the sensitivity test, the zonal boundary at  $47.0^\circ\text{N}$  is shifted to  $54.8^\circ\text{N}$ .

to be unrealistic, the test suggests that the adjacent fluxes, if source/sink pairs, may be overestimated in the absence of a buffer zone. The effect, even in this rather extreme case at  $47.0^\circ\text{N}$  is not large enough, however, to cause a significant challenge to our findings. There are almost no changes in the tropical and southern temperate fluxes caused by adding tropical buffer zones.

#### 4.3 Subdivision of zonal sources

Because we have limited the adjustable oceanic flux components to only three zones, and because the associated flux magnitudes are small relative to terrestrial biospheric flux magnitudes, shifting biospheric boundaries, as described in subsection 4.1 above, has a negligible oceanic influence, not further discussed here. We examine, however, the effect of installing oceanic boundaries between the temperate and polar zones one at a time in either hemisphere that match corresponding boundaries for the biospheric fluxes. In Figure 11 are shown the effects of a subdivision of the northern

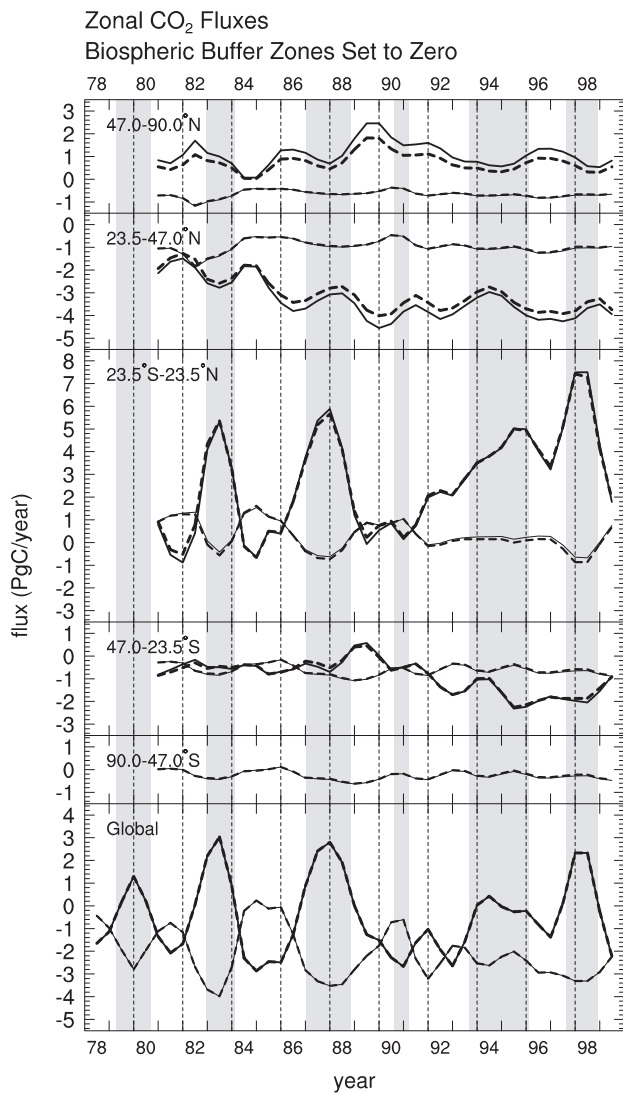


Fig. 10. Zonal fluxes, as in Figure 1, except that, for the sensitivity test, all terrestrial biospheric source components are set to zero in buffer zones between the boreal, temperate, and tropical zones. The width of each buffer zone is  $7.8^\circ$  ( $180/23$  degrees precisely) so that the nonzero flux in the boreal zone lies only between  $54.8^\circ$  N. and  $90^\circ$  N., in the temperate zones of each hemisphere between  $23.5^\circ$  and  $47.0^\circ$ , and in the tropical zone between  $15.6^\circ$  N. and  $15.6^\circ$  S.

adjustable oceanic source component of the standard case ( $23.5^\circ$  and  $90^\circ$ N.) at  $47^\circ$ N. In Figure 12 the effect of a similar division is shown for the southern hemisphere. In both sensitivity tests there are large opposing oceanic fluxes on either side of the installed boundary suggesting an unstable source configuration. Introducing a boundary at  $47^\circ$  alters the fluxes only of the bordering zones when introduced in the northern hemisphere, but when introduced in the southern hemisphere also affects the tropical flux. We conclude that our inverse procedure is not capable of resolving oceanic fluxes for more than one extratropical zone in each hemisphere.

We also examined the effect on the zonal fluxes of dividing the variable tropical biospheric source component, BIO2, into separate variable components for each hemisphere. The sum of the biospheric fluxes of the divided tropical zone, obtained by inversion, is almost identical to the tropical flux of the standard

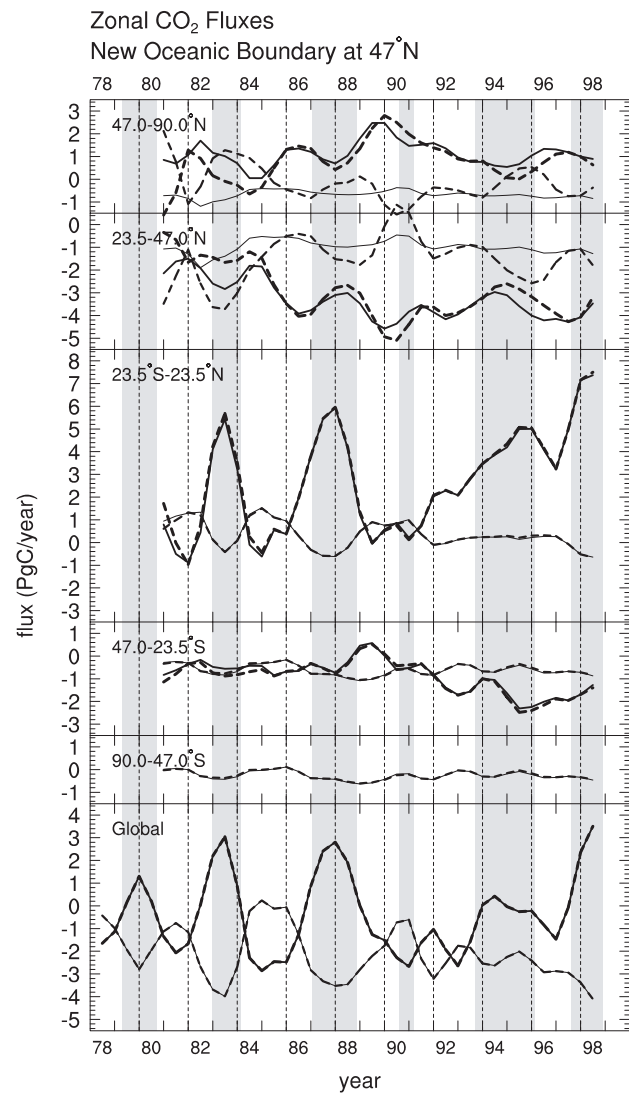


Fig. 11. Zonal fluxes, as in Figure 1, except that, for the sensitivity test, the adjustable northern oceanic source component, OCE3, is split into two zonal components at  $47^\circ$  N.

case, but the separate fluxes typically diverge from the sum by about  $2 \text{ PgC yr}^{-1}$ , with a difference in the extreme of nearly  $8 \text{ PgC yr}^{-1}$ . These large differences in flux correlate with small differences in the patterns of  $\text{CO}_2$  concentration and  $\delta^{13}\text{C}$  observed at individual tropical stations of our array, indicating that the calculation is too unstable to be useful in assessing the degree of actual similarity in patterns of the fluxes in the separate hemispheres.

Evidence that the patterns of flux in the two hemispheres are likely to be similar is furnished, however, by comparing tropical net primary production (NPP) for each hemisphere, calculated from a remotely-sensed vegetative index, NDVI as described in Article II, subsection A.10. The patterns in NPP, as discussed in subsection 7.1.2, below, are strikingly similar in the two hemispheres, a finding that is not surprising, because the El Niño phenomenon, which accounts for much of the variability in tropical plant growth, impacts the northern and southern tropics almost synchronously. Since variations in heterotrophic respiration are also likely to be caused largely by

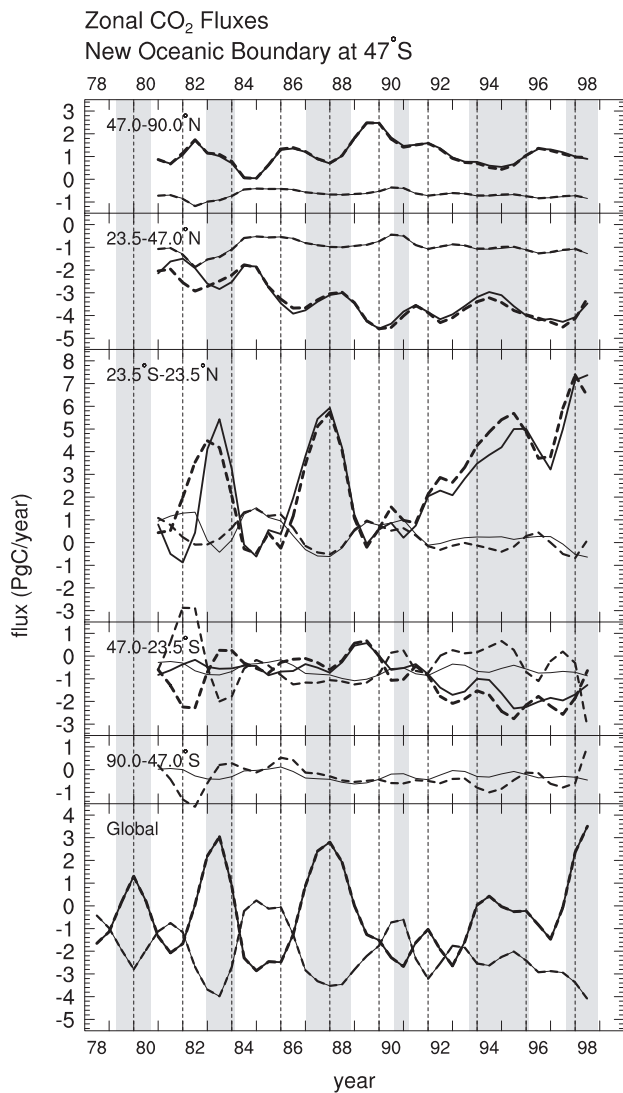


Fig. 12. Zonal fluxes, as in Figure 1, except that, for the sensitivity test, the southern oceanic source component, OCE1, is split at  $47.0^\circ$  S.

the El Niño phenomenon, variations in the net tropical fluxes should tend to be similar in the two hemispheres as well.

## 5. SENSITIVITY TO THE OBSERVATIONAL NETWORK

### 5.1 Christmas Island data excluded

In this test, in order to judge how crucial the observational record for Christmas Island is to our simulation of fluxes, both atmospheric  $\text{CO}_2$  concentration and  $^{13}\text{C}/^{12}\text{C}$  are excluded for this station in the inversion procedure. Data for this station, situated in the middle of the tropical Pacific Ocean at  $2^\circ\text{N}$ ,  $157^\circ\text{W}$ , might be expected to exert a large influence on the tropical fluxes that we infer. Also, the isotopic record is one of our longest, beginning in 1977. Nevertheless, if Christmas Island data are ignored, the major features of all of the regional fluxes are nearly the same as for the standard case (Figure 13), except early in the record when isotopic data are lacking for three or more other stations. After 1986, when all station records of our array furnish complete isotopic and concentration data, the differences in the oceanic and

biospheric fluxes from the standard case are generally less than  $0.3 \text{ PgC yr}^{-1}$ , except in the tropics, where the exclusion of observations at Christmas Island tends to increase slightly the interannual variability. In this test we did not recalculate the global constraints from the double deconvolution (see section 1, above) because the effect of omitting Christmas Island would have been negligible.

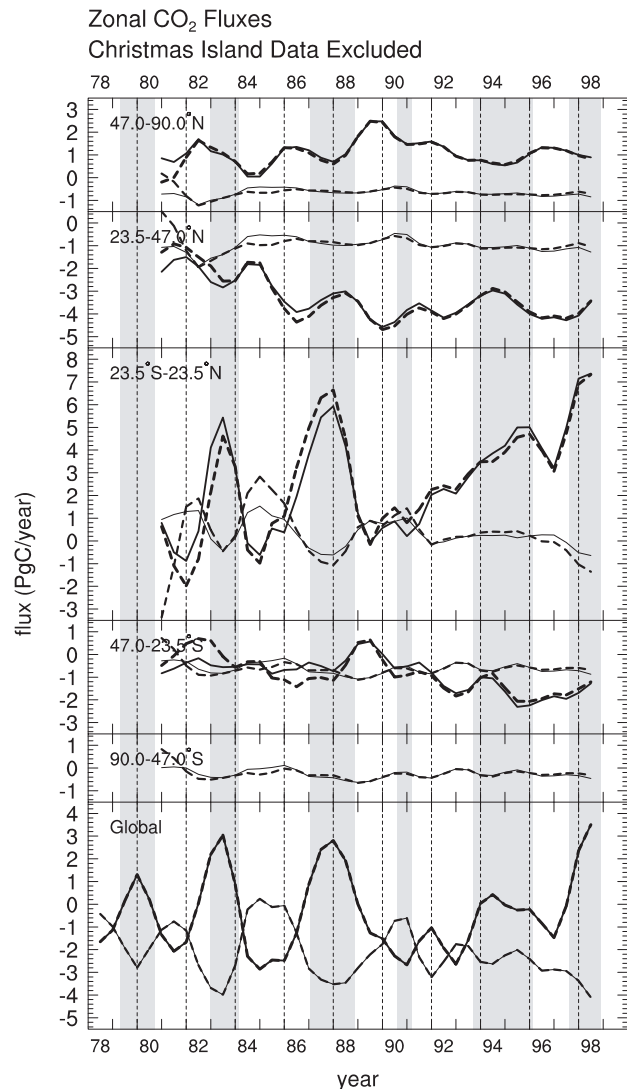


Fig. 13. Zonal fluxes, as in Figure 1, except that, for the sensitivity test, observations of  $\text{CO}_2$  concentration and  $^{13}\text{C}/^{12}\text{C}$  ratio for Christmas Island ( $2.0^\circ$  N.,  $157.3^\circ$  W) are excluded from the computations.

### 5.2 Inclusion only of complete data series

In our standard case, all available observational data are included at each time step, so that the number of stations providing data varies from 6 in 1981 to 9 in 1986 for  $\text{CO}_2$  concentration, and from 4 to 9 for  $^{13}\text{C}/^{12}\text{C}$ . To investigate the influence of the stations having incomplete records before 1986, we performed a test in which data for these stations is ignored, leaving concentration data for 6 stations, isotopic data for 4 (Figure 14). For biospheric fluxes, appreciable differences from the standard case are seen in the northern temperate

and boreal zones, a decrease in the boreal flux, up to  $0.8 \text{ PgC yr}^{-1}$ , approximately compensated for by a similar increase in the temperate flux. These differences are produced primarily by the exclusion of crucial  $^{13}\text{C}/^{12}\text{C}$  observations from Point Barrow at  $71^\circ\text{N}$ . The further exclusion of both concentration and  $^{13}\text{C}/^{12}\text{C}$  data from Alert at  $82^\circ\text{N}$ , however, has only a small effect on fluxes, because the data mainly just support those for Point Barrow. The exclusions of concentration and  $^{13}\text{C}/^{12}\text{C}$  data for Samoa ( $16^\circ\text{S}$ ) and Kermadec ( $29^\circ\text{S}$ ) and of  $^{13}\text{C}/^{12}\text{C}$  data from New Zealand ( $41^\circ\text{S}$ ) appear to have little effect on the flux calculations.

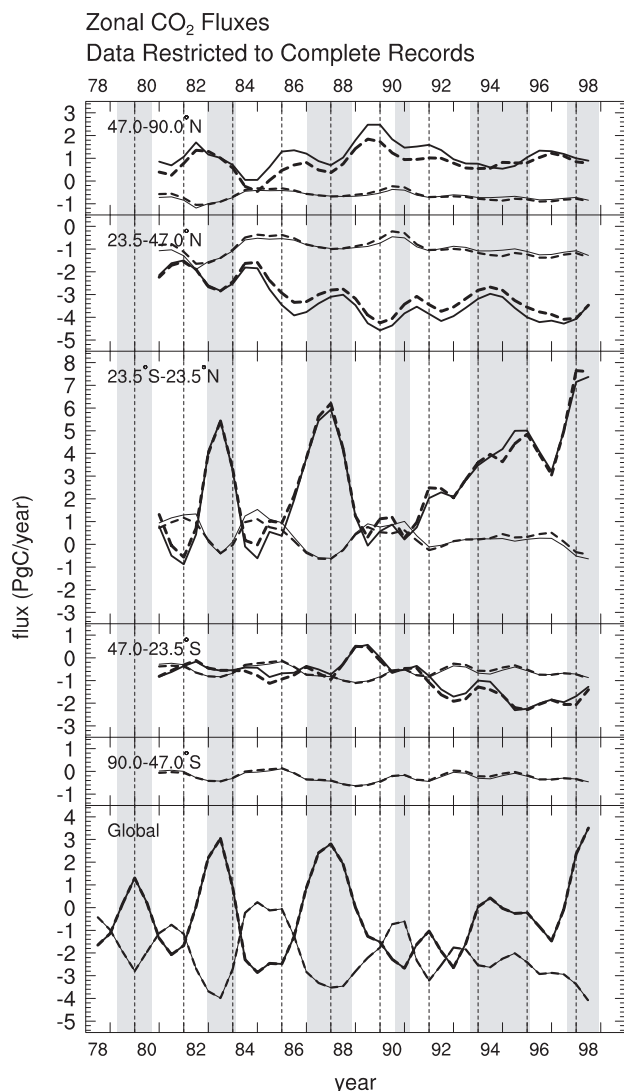


Fig. 14. Zonal fluxes, as in Figure 1, except that, for the sensitivity test, observations for stations having incomplete records are excluded from the computations. (Records are complete for concentration at PTB, LJO, KUM, CHR, NZD, and SPO; for  $^{13}\text{C}/^{12}\text{C}$  at LJO, KUM, CHR, and SPO. See Article I, Table 1, for interpretation of station codes.)

### 5.3 Alternative modeling of the La Jolla site

La Jolla, California, the only observing station in our array situated in the northern temperate zone, is critical in our study to the partitioning of fluxes in the northern hemisphere. The station poses special problems for modeling because, although

a coastal site where uncontaminated air from deep within the Pacific Ocean basin can be sampled every few days for at least a few hours, it is situated within an area affected most of the time by industrial  $\text{CO}_2$  emissions produced by the metropolitan areas of San Diego and Los Angeles and by inland terrestrial biospheric sources and sinks. These local to regional influences are largely avoided in our observational data by accepting only measurements made during steady onshore ocean winds, but in our standard case calculations of annual averages we have not similarly selected model results.

One approach for interpreting measurements at a coastal station selectively sampled like La Jolla is to assume that the data are characteristic of the air, say, one model grid box offshore. Indeed, weather maps, and a special sampling study [Lancaster, 1985], indicate that the air selectively sampled at our La Jolla station had recently been in or near the location of this grid box. Simulations in this offshore calculation (not shown) produce a ridiculously large northern temperate terrestrial biospheric sink because the predicted atmospheric  $\text{CO}_2$  concentration offshore is significantly higher than at the Pacific coast owing to the strong biospheric sink inland inferred by the standard case. An assumption that our data for La Jolla are valid offshore requires an even larger biospheric sink inland to predict the  $\text{CO}_2$  concentration at La Jolla.

In an alternative sensitivity test, the land-based industrial and terrestrial biospheric sources of the model were removed from the grid box in which La Jolla is located. This alteration has the advantage over the previous test of leaving the relationship of the station to the large-scale meteorological fields unchanged. As shown in Figure 15, Panel a, this test case causes large changes in inferred terrestrial biospheric fluxes averaged over the record period. The inferred northern temperate sink is diminished by  $1.7 \text{ PgC yr}^{-1}$ . In compensation, the boreal source is diminished by  $1.2 \text{ PgC yr}^{-1}$ , becoming a slight sink, and the tropical source is diminished by  $0.8 \text{ PgC yr}^{-1}$ . There is even a small  $0.2 \text{ PgC yr}^{-1}$  decrease in the southern temperate sink. The differences from the standard case for the boreal and north temperate fluxes increase over the record period, in proportion, more or less, to an increase in the northern temperate sink which survives from the standard case, though diminished by about a half.

In a variant on this test (Figure 15, Panel b), land-based terrestrial fluxes were removed from not only the grid box of La Jolla, but also from the grid box to the east, which also contributes to the model simulation of atmospheric  $\text{CO}_2$  at La Jolla because of the geographic interpolation scheme used (see Article II, section 3). In this test the northern temperate terrestrial biospheric sink increased by 0 to  $0.8 \text{ PgC yr}^{-1}$  from the case in which terrestrial fluxes were removed only from the La Jolla grid box. Evidently, the latter case predicts the least possible biospheric sink attainable at the coarse grid spacing used in our study.

If, in addition, the location of La Jolla is moved to the midpoint of the grid box, west by  $3^\circ$  and north by  $3^\circ$ , to remove the influence of terrestrial fluxes computed for neighboring grid boxes caused by our use of bilinear interpolation (see Article II, section 3), much of the drastic shift in fluxes is eliminated (Figure 16). Evidently the simulation of fluxes in

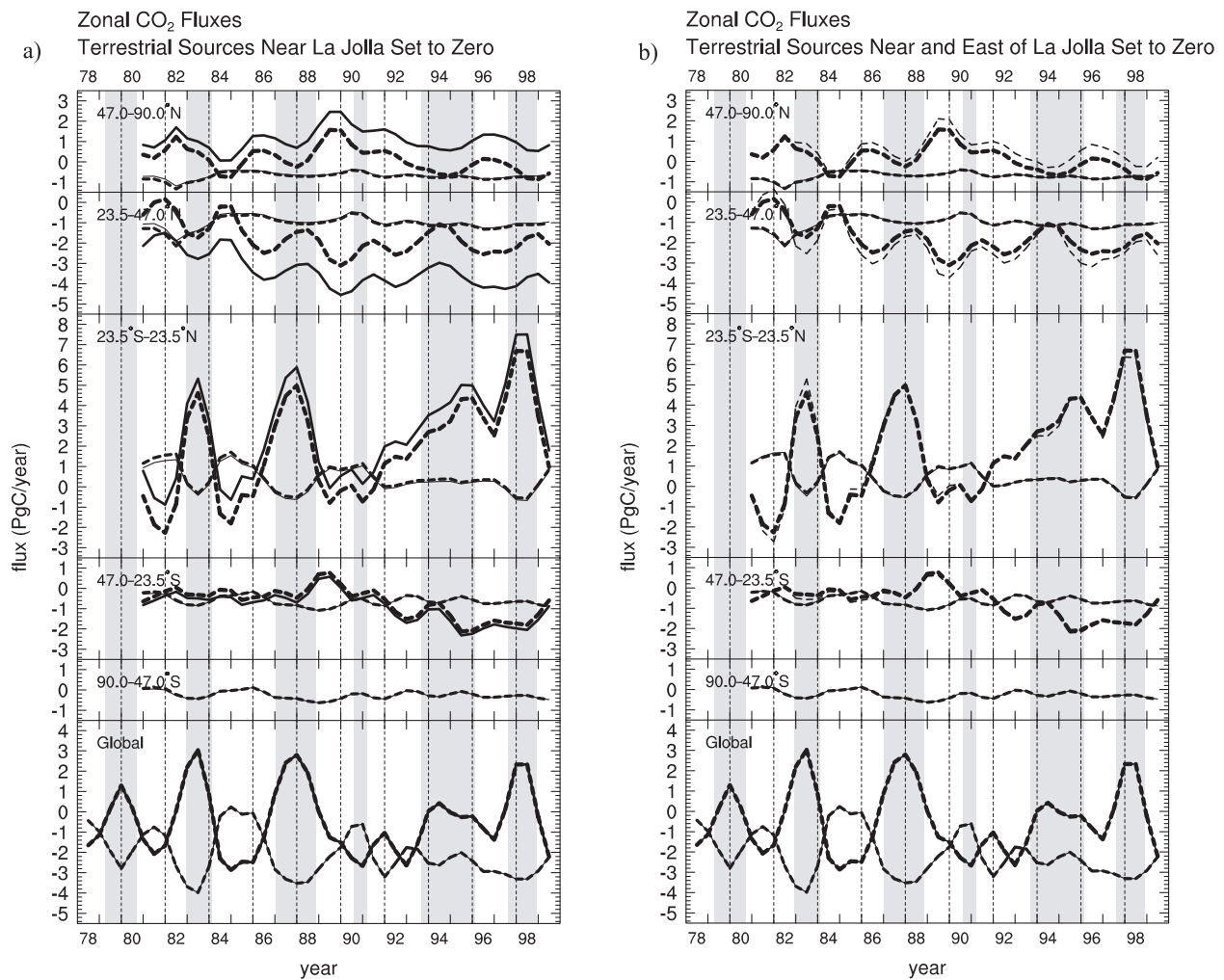


Fig. 15. Zonal fluxes, as in Figure 1, except that, for the sensitivity test, all terrestrial source components are set to zero in or near the La Jolla grid box. Elsewhere these components are readjusted, all by the same factor, to maintain the global totals of the standard case. **Panel a:** Components of La Jolla grid box set to zero (thick dashed line), compared with standard case (solid line). **Panel b:** Components set to zero within La Jolla grid box and also within the grid box to the east (thin dashed line), compared with the sensitivity case of Panel a (thick dashed line). As discussed in the text (subsection 8.4), the sensitivity test of Panel a has been selected provisionally as a preferred case.

the previous case is very sensitive to the exact location where strong biospheric and industrial sources still exist in the model. In this second modification, however, there is also an increased interannual variability in the northern temperate sink. This we attribute mainly to increasing industrial CO<sub>2</sub> production that occurred through the record period and progressive alteration of the relative contributions of these emissions and of biospheric fluxes inland of La Jolla.

Clearly it is more difficult to interpret data at a coastal site, such as La Jolla, when, frequently, strong local sources affect the CO<sub>2</sub> concentration at the measuring site. This difficulty does not apply to the chosen times of sampling, however, when the air is representative of deep Pacific Ocean air masses, but it does demonstrate a need to be able to predict the concentration field correctly close to the contact of these air masses with continental air having very different recent histories with respect to CO<sub>2</sub> sources and sinks.

To satisfy this need requires focusing on both short time-scales and on subgrid scales, which we have attempted to do to the extent that we have information. For 1986 and

1987, available meteorological fields for transport model TM2 allow a comparison of model predictions with the actual days of sampling. These predictions indicate a complicated relationship of transport to the major sources and sinks near La Jolla. The concentration of CO<sub>2</sub> predicted in the standard case for the model grid boxes of the La Jolla site and immediately to the west, show short-term fluctuations on the synoptic time scale [cf. Heimann et al., 1989, pages 299-300] of about 1 to 2 ppm, and up to 10 ppm for the grid box immediately to the east.

The days on which air samples were collected tend to match days having maxima in these fluctuations, contrary to our observations which occurred exclusively at times of minima. The discrepancy reflects the very different subgrid-scale distributions of the industrial and terrestrial biospheric CO<sub>2</sub> fluxes that largely determine fluctuations in the CO<sub>2</sub> concentration field for La Jolla. The industrial CO<sub>2</sub>, relative to the transport model's spatial scale of 7.8° by 10°, is concentrated near the sampling site, while the biospheric flux is diffuse and mostly remote in the northern portion of the grid

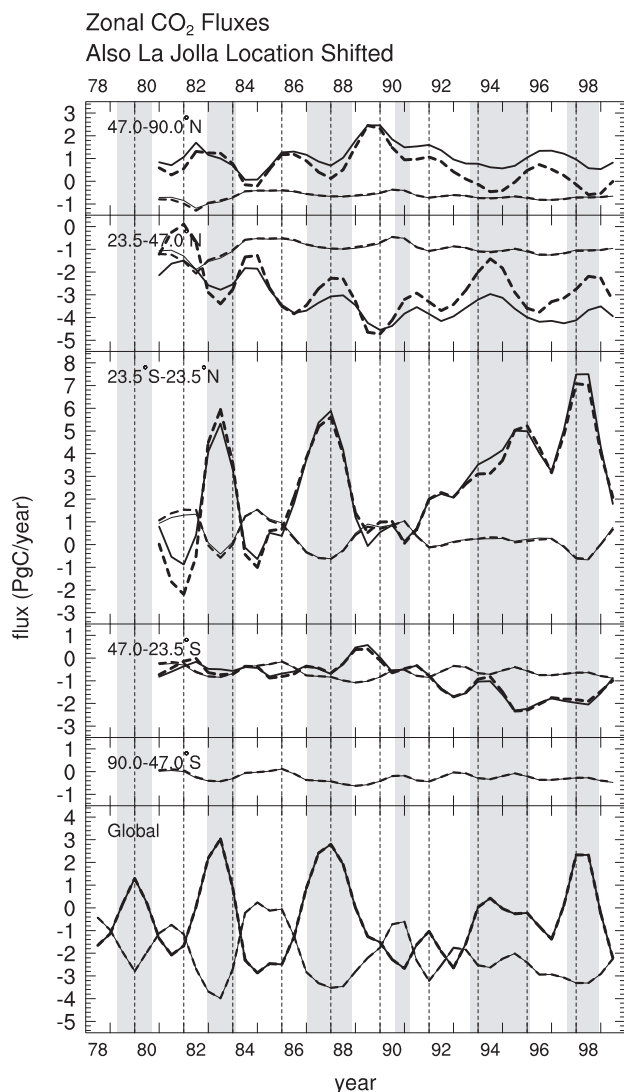


Fig. 16. Zonal fluxes, same as Figure 15, Panel a, except that the predicted concentration and  $^{13}\text{C}/^{12}\text{C}$  ratio of atmospheric  $\text{CO}_2$  for the gridbox (centered at  $35.22^\circ\text{N}$ ,  $120^\circ\text{W}$ .) are deemed to represent predictions for La Jolla, as though the station were situated at the midpoint of the box.

box. Also, the relative strengths of these two fluxes, critical to our calculations, differ from grid box to grid box, because of the bilinear interpolation used for predictions at exact station locations.

For the standard case, the strength of the industrial  $\text{CO}_2$  source of the La Jolla grid box is somewhat over twice that of the net biospheric sink, while the opposite relation holds for the grid box to the east. In the sensitivity test in which both terrestrial fluxes in the La Jolla grid box are eliminated, and, as a consequence of the new fit, the biospheric sink is reduced in the grid box to the east, there is a considerable difference in the proportion of industrial and biospheric fluxes affecting the La Jolla site, even though the predicted  $\text{CO}_2$  concentrations on the days of sampling still appear as maxima. In the second test in which, also, the La Jolla site is moved to the center of its grid box, thus eliminating the direct influence of the prediction for the grid box to the east, the relative influences of industrial and biospheric fluxes on the prediction

at La Jolla, is changed again. As a comparison of Figure 15 and 16 shows, the exclusion of the grid box to the east from consideration in the fitting procedure (second test) results in a substantially lower inferred north temperate biospheric flux than its inclusion (first test).

It is not obvious whether the standard case or one of the sensitivity test cases just described is most nearly correct. Atmospheric mixing is sufficiently strong that fluxes in areas farther from La Jolla than portrayed by neighboring grid boxes of TM2 also affect the  $\text{CO}_2$  concentration at the site. How far from the La Jolla grid box we should distort the programmed configuration of fluxes to compensate for the coarse scale in the transport model cannot be decided objectively at this time. Likewise, we cannot yet eliminate the shortcoming of our calculation that model predictions pertain to all days of the year whereas the observations are only for times of onshore winds when the air is not significantly affected by nearby terrestrial  $\text{CO}_2$  fluxes.

#### 5.4 Limited use of isotopic data

We have carried out several sensitivity tests in which we limited the use of  $^{13}\text{C}/^{12}\text{C}$  observations. As shown in Articles I and II, variations in atmospheric  $^{13}\text{C}/^{12}\text{C}$  observations produce variations in our simulated biospheric fluxes so large as to require substantial variations in the oceanic flux, nearly opposite in phase. However, these flux estimates rest on a possibly incorrect assumption that isotopic discrimination associated with photosynthesis of land plants is constant over time. In Article I, we argue that plant isotopic discrimination may vary in phase with El Niño events, decreasing during contemporary drought conditions at times shown approximately in our plots by vertical gray bars. By using only atmospheric  $\text{CO}_2$  observations in our inverse calculation to infer interannual variability in fluxes, we have carried out sensitivity tests in which variations in  $^{13}\text{C}/^{12}\text{C}$  can be attributed to causes not related directly to the magnitude of the biological flux, such as variable isotopic discrimination by plants.

In all of our calculations so far described, a global average of atmospheric  $^{13}\text{C}/^{12}\text{C}$ , estimated from our station observations, is used in a double deconvolution procedure (see Article I) to determine a global net biospheric flux. The same observations are used to establish annually averaged spatial  $^{13}\text{C}/^{12}\text{C}$  gradients to distinguish zonal biospheric and oceanic fluxes. As a sensitivity test, we exclude station observations of atmospheric  $^{13}\text{C}/^{12}\text{C}$  from both the zonal and global calculations.

If  $^{13}\text{C}/^{12}\text{C}$  data at both the global and local scales are disregarded, the inversion calculation is not stable, however, because the observing stations are not favorably located to allow biospheric and oceanic fluxes to be distinguished on the basis of atmospheric  $\text{CO}_2$  data alone. In order to stabilize this test calculation, we have set the three variable oceanic source components, OCE1, OCE2 and OCE3, constant at long-term average values determined in the standard case calculation, leaving only the 4 biospheric source components adjustable. Results of the test calculation are shown in Figure 17. There are still small variations in zonal oceanic fluxes produced

by prescribed oceanic source components that vary temporally in response to varying  $pCO_{2\ sea} - pCO_{2\ air}$ , because  $pCO_{2\ sea}$  varies with seasurface temperature in component OCD (see Article II, subsection A.3), and  $pCO_{2\ air}$  varies in accordance with observational data. These oceanic flux variations, however, are too small to affect significantly the calculation of the regional terrestrial biospheric fluxes, shown in the upper five panels. In the bottom panel are plotted global fluxes altered from the standard case, because the global oceanic flux (thinner dashed line) in this sensitivity test varies only in response to temperature change. The global terrestrial biospheric flux (thicker dashed line) is the difference between this flux and the sum of the oceanic and biospheric fluxes, unchanged from the standard case.

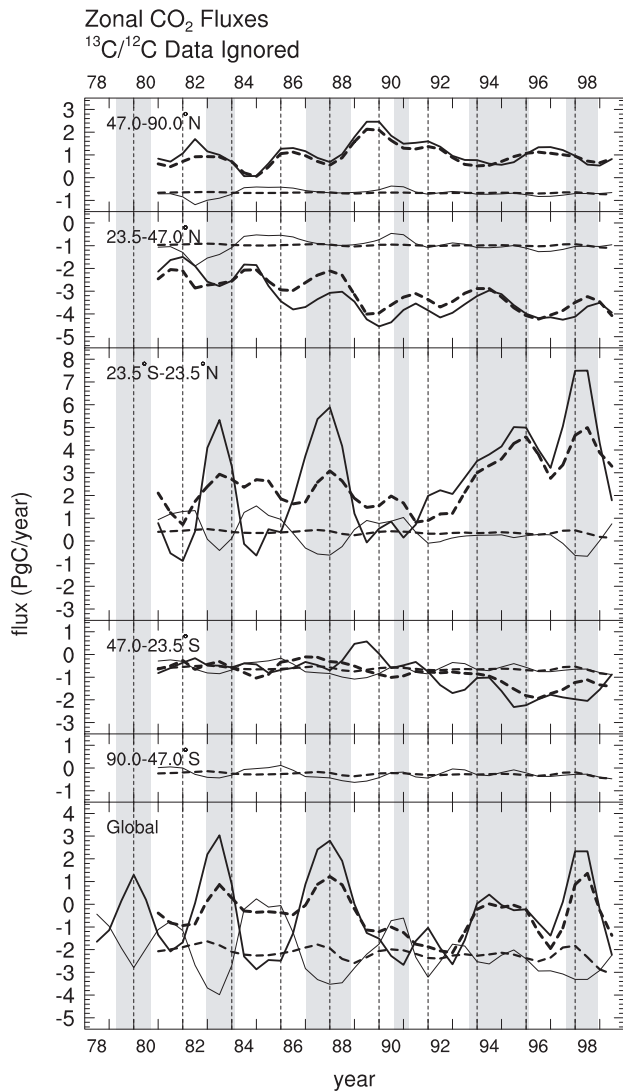


Fig. 17. Zonal fluxes, as in Figure 1, except that, for the sensitivity test,  $^{13}C/^{12}C$  data are used only to establish full record (19-year) averages of the three adjustable oceanic source components, forced in this sensitivity test to be time-invariant. Also, shown in the bottom panel, is the global oceanic flux (thinner dashed black line) and the global terrestrial biospheric flux (thicker dashed black line). The sum of these two fluxes is forced, as a global constraint, to be equal to the sum of the global fluxes of the standard case, each being the sum of the respective regional fluxes.

In the boreal zone, disregarding  $^{13}C/^{12}C$  data, the terrestrial

biospheric flux is almost identical to that of the standard case, indicating that the  $^{13}C/^{12}C$  data are not critical to establishing the patterns of variation there. In the two temperate zones, the biospheric flux is somewhat altered, especially in the southern hemisphere where the interannual variability, already small for the standard case, is almost negligible in the test case except near the end of the record. In the tropics, some of the biospheric flux of the standard case appears to have been shifted to the northern temperate sink, but of paramount significance is that the large interannual fluctuations of the standard case are substantially reduced. Forcing the tropical oceanic flux to be nearly constant in this test requires that the biospheric flux variation decrease in order to preserve the variation of the combined biospheric and oceanic tropical fluxes needed to agree with  $CO_2$  observations.

### 5.5 Limited use of all atmospheric $CO_2$ data

A striking finding of this study is the strong similarity of zonal terrestrial biospheric and oceanic net  $CO_2$  fluxes in the tropics to their global counterparts. This similarity is not just a consequence of the large proportion of global NPP assigned to the tropical zone of our model, because the inversion calculation senses only imbalances, not necessarily correlated with total NPP. The main factors that determine the degree of the similarity are the extent to which the observed patterns in  $CO_2$  concentration and  $\delta^{13}C$  at each station are similar to their global counterparts, and the character of atmospheric transport. To aid in examining the importance of these factors, we have carried out a sensitivity test in which the temporal variability for concentration and  $\delta^{13}C$  at every station of our array is set to be identical to the corresponding global patterns, without altering their averages over the period of complete records, 1986-1999, thus maintaining the same average north-south profiles.

If all zonal variability in atmospheric  $CO_2$  is suppressed, inferred patterns of the tropical terrestrial biospheric and oceanic fluxes, as shown in Figure 18 (thicker and thinner dashed lines, respectively), still show strong similarity to patterns in the global fluxes, whereas the extratropical terrestrial biospheric fluxes are less similar. Indeed, the biospheric flux in the northern temperate zone shows little variability at all. The extratropical oceanic fluxes, which in the standard case show patterns similar to their global average, are only slightly changed. These tropical versus extratropical differences, most evident in the biospheric fluxes, evidently reflect the character of the atmospheric mass transport, for which the most notable feature is the vigor of the tropical transport owing to the Hadley circulation [see plots, e.g. by Heimann and Keeling, 1989, Figure 1]. Atmospheric signals in concentration and  $\delta^{13}C$  produced by the tropical fluxes are readily propagated both vertically and meridionally, so that these signals are readily observed at all latitudes. As shown in the above cited figure [*loc. cit.*, Figure 1], the zonally averaged mass stream function is much weaker poleward of about  $35^\circ$  in each hemisphere, so that the extratropical signals are less broadly propagated than tropical signals. Indeed, if this sensitivity test is correct, practically no variation in biospheric flux within

the northern temperate zone is required to explain the pattern of atmospheric  $\text{CO}_2$  variation in this zone. That the Hadley circulation provides a barrier to mixing across the equator has little effect on this analysis, because the tropical patterns are similar in each hemisphere, as noted in subsection 4.3, above.

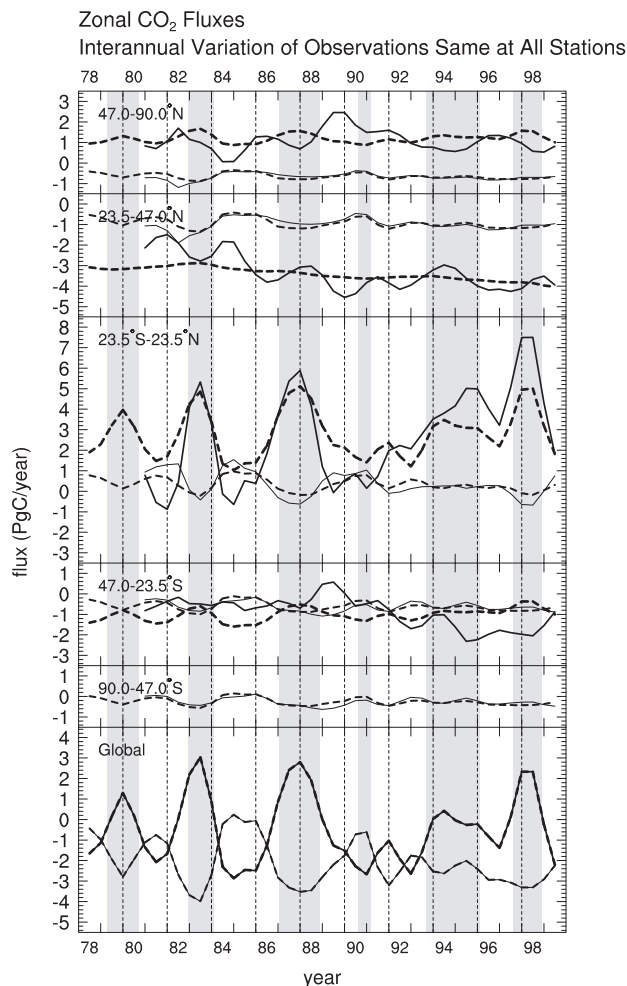


Fig. 18. Zonal fluxes, as in Figure 1, except that for the sensitivity test the concentration and  $^{13}\text{C}/^{12}\text{C}$  reduced isotopic ratio,  $\delta^{13}\text{C}$ , of each station record is assumed to vary from its mean of 1986 through 1999 by the 9-station global averages as listed, respectively, in Article I, Appendix D, Tables D3 and D4. (The global fluxes of this test, shown in the bottom panel, are very slightly changed from the standard case because of the averaging process used).

The extent to which interannual regional variations in flux can influence the observed patterns in atmospheric  $\text{CO}_2$  is shown in Figure 19 in which the simulated atmospheric patterns of the test case are compared with the standard case for four stations of our array. The largest departures, 0.7 ppm and 0.04‰, are seen in the far north. These departures in signals are no more than a few times the standard error of annual averages of the measurements (see Article I, Appendix D, Table D.3), a strong argument for striving to obtain the most precise atmospheric  $\text{CO}_2$  measurements possible for use in inverse studies.

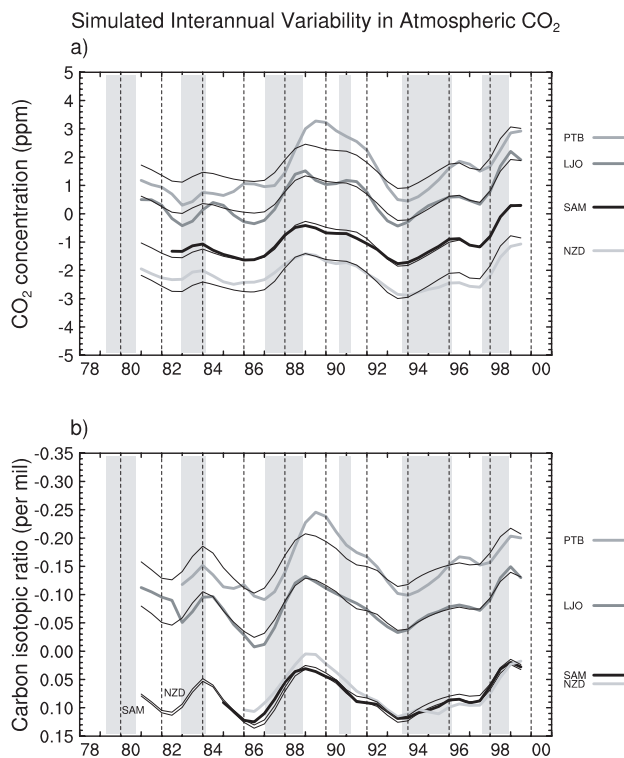


Fig. 19. Comparison of atmospheric  $\text{CO}_2$  concentration, in ppm, and its  $^{13}\text{C}/^{12}\text{C}$  reduced isotopic ratio,  $\delta^{13}\text{C}$ , in ‰, as simulated by the sensitivity test of Figure 18 (thick lines) and by the standard case (thin lines). Plots are shown for Point Barrow, Alaska (PTB, 71° N.), La Jolla, California (LJO, 33° N.), Samoa (SAM, 14° S.), and New Zealand (NZD, 41° S.), stations that display distinctly different mean values providing clarity in plotting. The largest departures in temporal variability from the standard case are for northern stations, two of which are shown in the plot. **Panel a:** concentration data. **Panel b:**  $\delta^{13}\text{C}$ .

## 6. SENSITIVITY TO INTERANNUAL VARIABILITY IN PRESCRIBED COMPONENTS

### 6.1 Industrial $\text{CO}_2$ component

The industrial flux of  $\text{CO}_2$  produced by the combustion of fossil fuel is comparable in magnitude to the fluxes of  $\text{CO}_2$  released by the terrestrial biosphere and the oceans. To establish these latter fluxes by inverse calculations therefore requires a precise accounting for the release of  $\text{CO}_2$  from combustion. As detailed in Appendix A of Article II (Section A.2), we have used compilations for 1980 and 1990 of Andres et al. [2000] to specify the spatial distribution of this source together with a small additional source from cement manufacture. As this compilation indicates, a substantial southward shift in industrial emissions occurred over the 1980's. In our standard case, lacking better information, we projected continuing shifts at the same rate after 1990 for each 8° by 10° box of our inverse model.

We cannot characterize errors in the distribution of industrial  $\text{CO}_2$  emissions precisely, but with a sensitivity test we illustrate that the errors possibly are not trivial. As shown in Figure 20, we have compared our standard scenario of emissions, shown by solid lines for each zone, with an alternative scenario, shown by dashed lines. The latter for 1995 uses the same annual global emission totals, but is distributed on the basis of a new estimate of population within countries developed

by Li [1996] and of different assigned carbon contents for coal [Brenkert et al., 1998], resulting in a greater southward shift in emissions from 1990 to 1995 than our standard case provides. Beyond 1995, we assumed no further change in distribution. The differences in flux for the two scenarios result in substantial changes in the inferred boreal and northern temperate terrestrial biospheric fluxes in the 1990's, as shown in Figure 21. The flux increases north of 47°N by up to 0.7 PgC yr<sup>-1</sup>, and decreases to the south in the adjacent temperate zone by up to 1.0 PgC yr<sup>-1</sup>. A small increase in the biospheric flux occurs in the tropics. The oceanic fluxes are almost unchanged in all zones, because our model calculations take into account that the isotopic signature of fossil fuel CO<sub>2</sub> is nearly the same as for terrestrial biospheric carbon and therefore has little effect on the calculation of these fluxes.

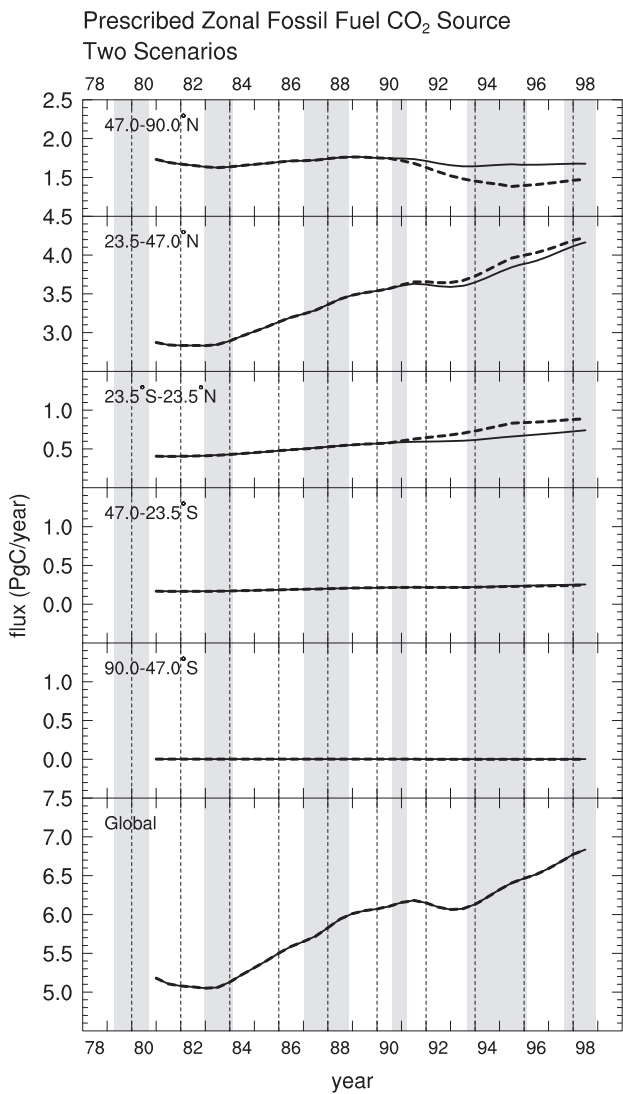


Fig. 20. Comparison of the distribution of industrial CO<sub>2</sub> emissions, in PgC yr<sup>-1</sup>, used for the standard case calculation of zonal fluxes (solid lines), with an alternative distribution (dashed lines) in which emissions after 1990 are decreased in the northern zones and increased in the tropical zone, as described in the text, keeping the same global totals.

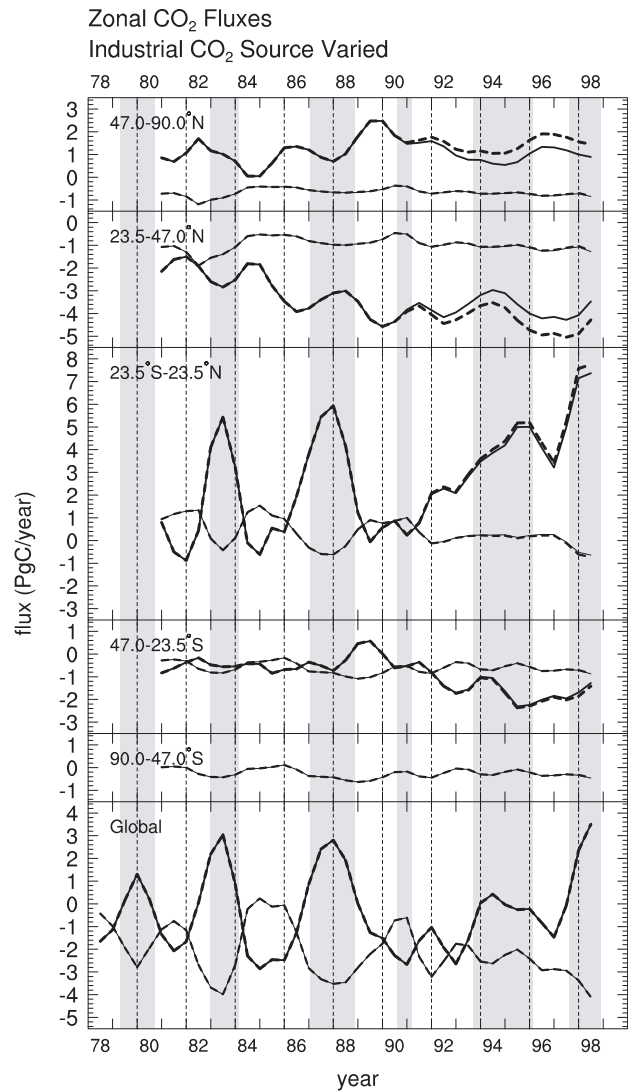


Fig. 21. Zonal fluxes, as in Figure 1, except that, for the sensitivity test, industrial CO<sub>2</sub> emissions are increased southward in the 1990's, as shown in Figure 20.

### 6.2 Net primary production

Because reliable NDVI vegetative index data are not available over the entire period of our study, we have calculated net primary production (NPP) mainly to establish an average seasonal cycle based on data from 1982 through 1990, as discussed in Article II, subsection A.10. Here we make use of the full data set of available NDVI data to compute fluxes that vary interannually in response to observed changes in NDVI. All other aspects of the calculations remain the same as the standard case. As seen in Figure 22, the departures from the standard case are not significant. This is because the terrestrial biospheric source components depend on NPP only to establish source patterns within each biospheric zone. These patterns do not vary significantly over the NDVI record period.

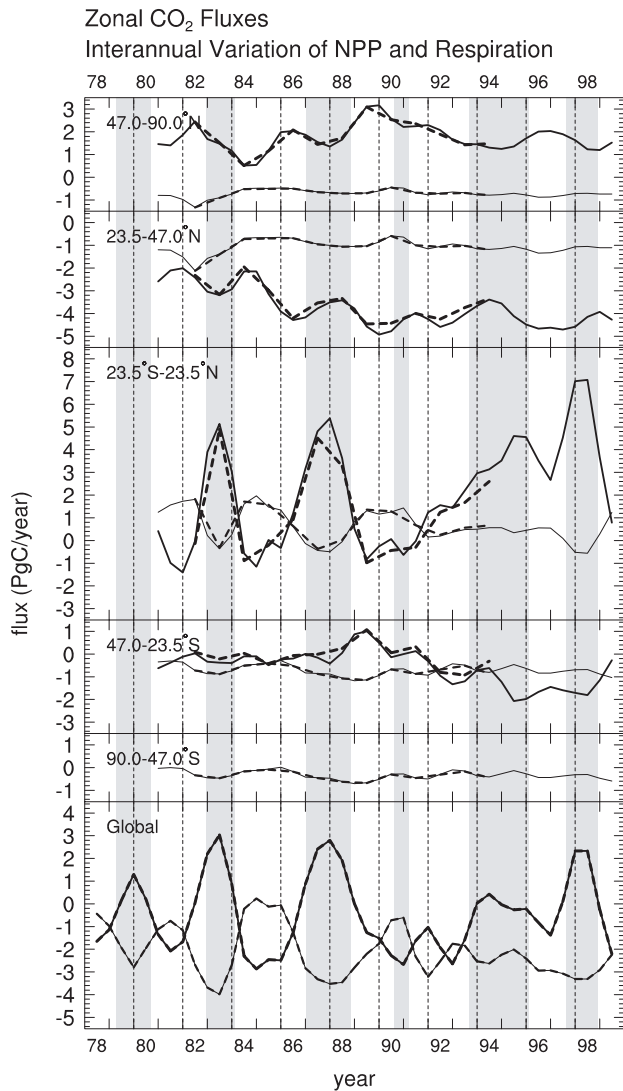


Fig. 22. Zonal fluxes, as in Figure 1, except that for the sensitivity test (dashed lines) net primary production of land plants (NPP) varies from year to year according to a normalized difference vegetative index (NDVI), whereas NPP is used in the standard case only to establish an interannually fixed seasonal cycle based on data averaged from 1982 through 1990. The sensitivity test takes into account only the source components for NPP and heterotrophic respiration, described in Article II, subsection A.10. Also, 1987 winds were used in this calculation, and on this account comparison is made to the sensitivity test case of Figure 1 (solid lines). The global fluxes, shown in the bottom panel, are unchanged from the standard case, because their calculation does not depend on NPP or wind data.

## 7. SENSITIVITY TO SELECTED ASPECTS OF THE $^{13}\text{C}/^{12}\text{C}$ MODEL

### 7.1 Modeling of C3 and C4 plants

**7.1.1 Influence of C4 plants:** A large difference in carbon isotopic discrimination between C3 and C4 plants during photosynthesis (about 18‰ for C3 plants, 4‰ for C4 plants) causes zonal average discrimination to vary, because the fraction of net primary production (NPP) owing exclusively to C3 plants varies spatially (Article I, subsection 5.10). This zonal variability, accounted for in our standard case (Article I, Table 6), is ignored in the sensitivity test described here by prescribing discrimination everywhere to be about 18‰,

as assumed by Heimann and Keeling [1989] and Keeling et al. [1995]. This changed prescription applies globally to the double deconvolution procedure as well as regionally. As Figure 23 indicates, the largest differences from the standard case are smaller fluctuations in the tropical biospheric flux. Inferred peak fluxes, near times of El Niño events, are reduced by about  $1.0 \text{ PgC yr}^{-1}$ .

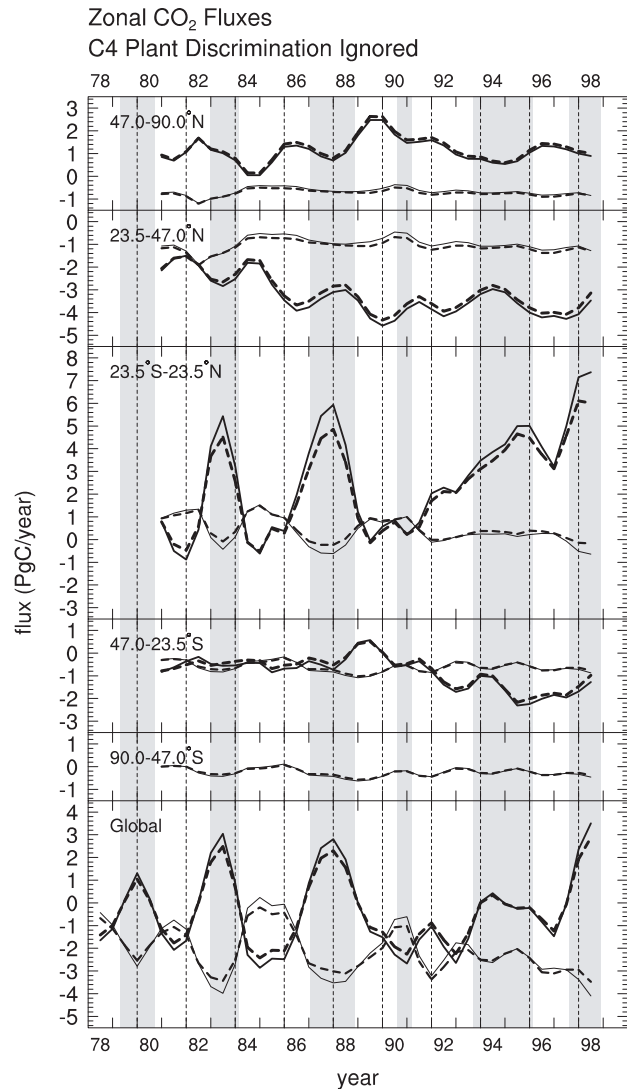


Fig. 23. Zonal fluxes, as in Figure 1, except that, for the sensitivity test, net primary production of the terrestrial biospheric source components is assigned everywhere the isotopic discrimination representing the global average for C3 plants, whereas, in the standard case, for each geographic zone, lower discrimination of C4 plants is also accounted for. This alternative discrimination is also implemented in the deconvolution used to calculate global constraints, producing differences in global fluxes from the standard case, shown in the bottom panel.

**7.1.2 Temporal variations in isotopic discrimination of plants:** Carbon isotopic discrimination associated with photosynthesis, in addition to being zonally variable, as discussed above, may vary temporally (Article I, section 5), although to what degree is not known. Exclusively seasonal variability in discrimination will not be discussed here, because it does not significantly affect our simulations of annual average fluxes. Interannual variability, however, may be important. In

our standard case, discrimination was held constant because reliable information on variability was not available. One line of direct evidence lends some support for this assumption with respect to temporal variability in discrimination that could be caused by changes in the proportions of contributions from C3 and C4 plants. We have calculated NPP on a  $1^\circ$  by  $1^\circ$  grid from a normalized difference vegetative index (NDVI) of plant activity, distinguishing areas of predominantly C3 and C4 plants (Article II, subsection 4.2). As shown in Figure 24, Panel a, NPP in the tropical zone, on this fine grid scale, varied almost proportionally for C3 and C4 plants. (As a precaution in this interpretation, we note that in calculating NPP a constant quantum efficiency factor and PAR from a single year are used. We cannot confirm that interannual variations in the efficiency factor or in PAR are negligible.) In Figure 24, Panel b, NPP of combined C3 and C4 plants is shown separately for the northern and southern hemispheres. The data, obtained from the same calculations of NPP as in the plots of Panel a, show very similar patterns, indicating that the variations in NPP for both types of plants are nearly the same in both hemispheres.

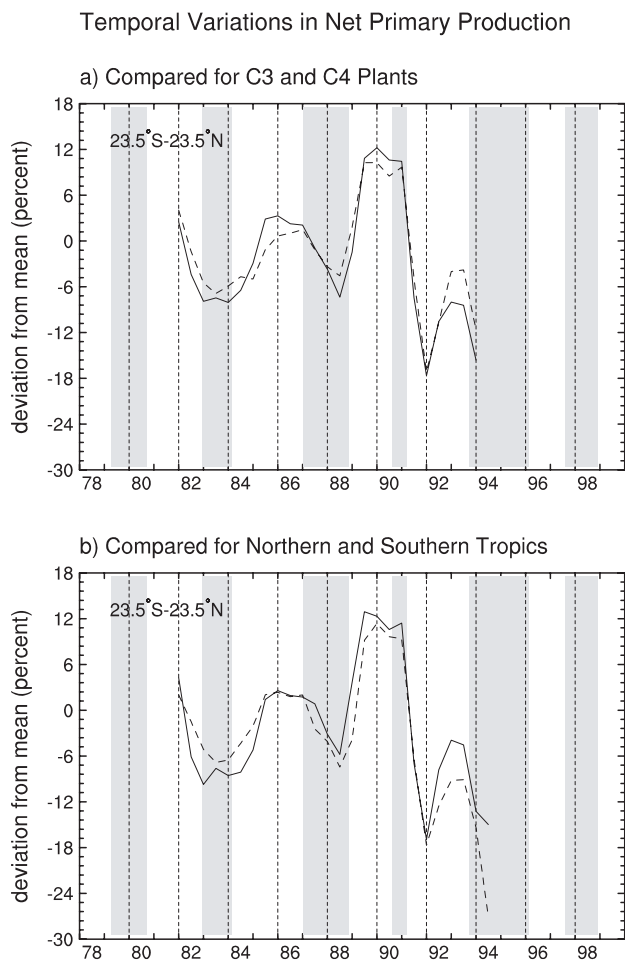


Fig. 24. Interannual variation, expressed as percentage departures from average, in net primary production (NPP) in the tropical zone,  $23.5^\circ$  N. to  $23.5^\circ$  S. with respect to plant type and hemisphere. **Panel a:** C3- versus C4-plant biomes (solid and dashed lines, respectively). **Panel b:** NPP of both C3- and C4-plants in the northern versus southern hemisphere (solid and dashed lines, respectively). Mean annual NPP for 1982-1990 was  $24.0 \text{ PgC yr}^{-1}$  for C3 plants,  $8.8 \text{ PgC yr}^{-1}$  for C4 plants,  $14.1 \text{ PgC yr}^{-1}$  for northern hemisphere, and  $18.7 \text{ PgC yr}^{-1}$  for southern hemisphere.

Interannual variability in discrimination *per se* is more difficult to establish, but more likely to exist and to impact our calculations. We have some evidence of the degree of variability for C3 plants in the temperate and boreal zones during the 1990's, based on the covariance of the seasonal cycle of  $\text{CO}_2$  concentration and  $^{13}\text{C}/^{12}\text{C}$  ratio (Article I, section 3). Greater inferred discrimination, by as much as 2%, is indicated near times of El Niño events. If discrimination of tropical C3 plants should similarly vary, the magnitude of fluctuations that we infer for the tropical net biospheric flux would be even larger than when assuming constant discrimination. In Article I and again in Article IV, we suggest, however, that for tropical C3 plants lesser discrimination may occur near times of El Niño events because of more prevalent drought, and that neglecting to take this possibility into account may have led to predicting fluctuations of biospheric fluxes that are too large. We have no data to verify or refute this possibility, but it appears more likely to be valid only for the tropics. The degree and timing of variability in discrimination thus remains an unresolved issue.

## 7.2 Exclusion of the oceanic source component for temperature-dependent isotopic fractionation

We have investigated the effect on our model simulations of the oceanic temperature-dependent fractionation source component, TDF. This source component, described in Article II, subsection A.9, produces a larger north-south gradient in annually-averaged atmospheric  $^{13}\text{C}/^{12}\text{C}$  in the southern hemisphere (more negative  $\delta^{13}\text{C}$  southward) than any other component. As a drastic sensitivity test, the TDF source component was excluded entirely. The strongest change in inferred fluxes, as shown in Figure 25, is to increase the southern temperate biospheric source by the order of  $2 \text{ PgC yr}^{-1}$  while decreasing the tropical biospheric source and to a small degree increasing the northern temperate sink. These shifts in flux are expected, since the atmospheric  $^{13}\text{C}/^{12}\text{C}$  gradient produced by the TDF source component (increasingly negative southward in the southern hemisphere) is strongest across the southern temperate zone. Also seen in Figure 25 are decreases in the zonal oceanic fluxes in the southern hemispheric temperate and polar zones and increases in the tropics and northern hemisphere, reflecting the far stronger poleward increases in  $^{13}\text{C}/^{12}\text{C}$  of the TDF component in the southern hemisphere than in the northern. Interannual variations in fluxes are in all cases similar to those in the standard case, since the TDF component is assumed to be temporally invariant.

Interannual variability in sea surface temperature and wind speed in the TDF source component is not accounted for in our standard case calculation, but is expected to be small. The latitudinal gradients in  $^{13}\text{C}/^{12}\text{C}$  result from differences of more than  $20^\circ\text{C}$  between the polar and tropical oceanic surface waters. Interannual variations in zonally averaged temperature are likely to be much smaller, of the order of  $1^\circ\text{C}$ , too small to be significant to our calculations. Interannual variations in wind speeds, which affect the relative rates of air-sea  $\text{CO}_2$  exchange between zones, are likewise probably small when averaged zonally.

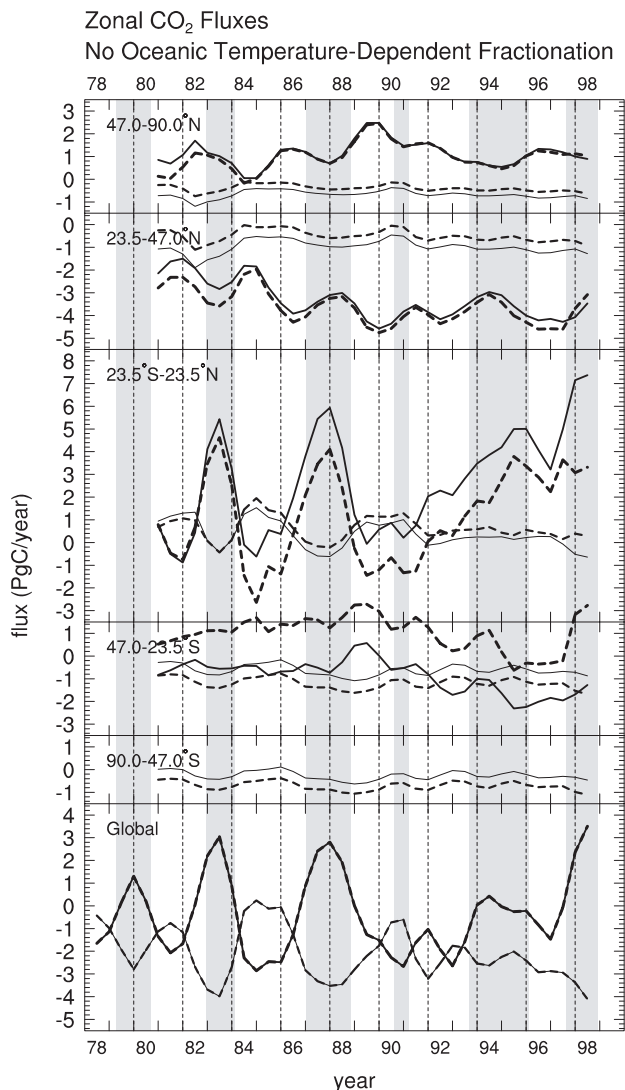


Fig. 25. Zonal fluxes, as in Figure 1, except that, for the sensitivity test, the oceanic source component for temperature-dependent fractionation (TDF) is excluded.

### 7.3 Isotopic signature of fossil fuel emissions

Here, we investigate the sensitivity of the inverse calculation to the isotopic signature of fossil fuel emissions. In our standard case calculation, an average  $^{13}\text{C}/^{12}\text{C}$  ratio for fossil fuel was used, based on work of Andres et al. [2000]. This isotopic signature, about  $-28\text{‰}$ , relative to the international isotopic standard, PDB, differed from that in the earlier study of Keeling et al. [1989] by about  $1\text{‰}$ . We have verified in a calculation (not shown) that this revision, a 5 percent change in difference from the atmospheric value of about  $-8\text{‰}$ , does not produce a significant change in the inferred fluxes (also see Ciais et al. [1995], Figure 14).

Data on spatial variations in the isotopic signature of fossil fuel emissions became available recently, but not in time to be incorporated in our calculations except in a sensitivity test. Andres et al. [2000] present latitudinally averaged compilations for 10 year intervals from 1950 to 1990, and for 1991 and 1992. For 1990, the isotopic signature varied over a wide range of about  $-25$  to  $-33.5\text{‰}$  averaged for 1 degree latitudinal bands,

with more negative values in the tropics and high latitudes, separated by more positive values in the subtropics. Over the narrower latitudinal zone from  $25$  to  $55^\circ\text{N}$ , however, where significant emissions of fossil fuel occur, there is a smaller range, decreasing from about  $-27\text{‰}$  in the south to about  $-31\text{‰}$  in the north. The compilation shows that this north-south gradient increased from 1980 to 1992 by about  $2.5\text{‰}$ . We have verified that these changes in  $^{13}\text{C}/^{12}\text{C}$  (not shown) have a negligible effect on our calculations.

## 8. DISCUSSION AND CONCLUDING REMARKS

### 8.1 Introduction

With sensitivity tests, we have sought to establish whether our choices of carbon cycle model characteristics and of observational data produce reliable estimates of regional exchanges of atmospheric  $\text{CO}_2$  with the terrestrial biosphere and the oceans. This spectrum of tests is broad enough to reveal important uncertainties in the  $\text{CO}_2$  fluxes inferred from measurements of the concentration and the  $^{13}\text{C}/^{12}\text{C}$  isotopic ratio of atmospheric  $\text{CO}_2$ , but also to identify important features of our calculations that are robust. We now summarize the results of these tests relative to a standard case adopted *a priori*, identifying errors pertaining to the full record period of 19 years and also to shorter time-scales. Also, we select, *a posteriori*, a "preferred case" more likely than the standard case to represent regional biospheric and oceanic fluxes correctly, as discussed in subsection 8.4, below.

The biospheric and oceanic net exchange fluxes of  $\text{CO}_2$  that we infer from inverse calculations are constrained to sum each year to global values determined by double deconvolution, which are uncertain to about  $1.0 \text{ PgC yr}^{-1}$  at 90% confidence, including biases (Article I, Table 7, and Article IV, subsection 5.4). Being spread over 4 terrestrial and 3 oceanic zones, they contribute only small uncertainties to our calculation of zonal fluxes. They are subject, however, to statistical errors estimated on the basis of scatter in our atmospheric  $\text{CO}_2$  concentration and  $^{13}\text{C}/^{12}\text{C}$  data to be  $1.0 \text{ PgC yr}^{-1}$  (expressed at 2 sigma, see Article II, Figure 6).

After accounting separately for the global  $\text{CO}_2$  source from combustion of fossil fuels, our standard case calculation indicates that individual zonal fluxes have generally remained predominantly either sources or sinks of atmospheric  $\text{CO}_2$  over the past 20 years. Our most secure finding depends on atmospheric  $\text{CO}_2$  data alone: that the terrestrial biosphere and oceans in combination produce a sink of atmospheric  $\text{CO}_2$  in the northern temperate zone and most of the time a source of atmospheric  $\text{CO}_2$  in the tropics. Also, not challenged by this study, is a global oceanic sink required as a response to persistently rising atmospheric  $\text{CO}_2$  concentration. Taking account of  $^{13}\text{C}/^{12}\text{C}$  isotopic data, we find that both the tropical terrestrial biosphere and the tropical oceans are inferred to be sources, the extratropical oceans, therefore, surely sinks. Also the terrestrial biosphere is a strong sink in the northern temperate zone. The terrestrial biosphere in the boreal zone and in the southern temperate zone are sometimes sources, sometimes sinks.

By our sensitivity tests, we have challenged the standard case calculations of fluxes, taking note that the strengths of

the inferred biospheric fluxes are generally greater than of the oceanic fluxes and vary considerably more from one sensitivity test to another. Here we first consider the goodness of fit of the calculation of fluxes and then the extent to which individual biospheric fluxes, simulated by the inversion model, varies from test to test. For the northern temperate zone, we also consider whether the simulated biospheric sink there is implausibly large compared with net primary production (NPP).

### 8.2 Chi-square test of goodness of fit

A useful criterion in evaluating sensitivity tests is the goodness of fit expressed by a reduced chi-square, described in Article II, subsection 6.2. We have computed this statistical measure of the likelihood that the model is consistent with the input data, as listed in Table 2, averaged from 1986, when we first have data for all stations to 1989, and also to the end of 1998. In addition, averages just for the 1990's are provided to aid comparison with other recent studies. We now summarize these results quoting chi square values for 1990-1998 (see Addendum, below).

Values of chi square sharply higher than the standard case (4.28) are found when oceanic temperature dependent isotopic fractionation is ignored (10.44) and when the northern temperate biospheric flux is set to zero (15.31), effectively ruling out these possibilities. Substituting 1987 or 1998 winds for 1986 winds causes higher values (5.08, 6.16, respectively), suggesting that the winds for 1986 are more representative for the entire record period than the substituted winds of the two test cases. For the test employing interannually varying winds, we are limited to comparisons before 1994. Moreover, chi-square for 1990, 1992, 1993 in this test case are exceptionally poor. Restricting the comparison to the period from 1983 through 1989, chi-square of the test case (7.25) is almost the same as for the standard case (7.16 for this period).

If only concentration data are used in the fitting procedure, chi-square is diminished (3.76), owing to their greater precision than that of isotopic data. Using all atmospheric data, but only for stations with long records, leads to a low chi-square (3.16), probably because the number of stations hardly exceeds the number of zones defined in the inversion model. Perhaps for the same reason, chi-square is slightly lower when data are excluded just for Christmas Island (4.10). Surprisingly, ignoring C4 plant discrimination leads to a lower chi-square (3.88).

A sensitivity test in which terrestrial sources are removed from the La Jolla grid box produces a poorer fit (4.80) than the standard case, a still poorer fit if also removed from the next box to the east (5.05). The first of these tests is moderately improved if La Jolla is also assumed to be at the center of the grid box (4.40). All three tests result in poorer predictions of the gradients of CO<sub>2</sub> concentration and <sup>13</sup>C/<sup>12</sup>C between La Jolla, California, and Cape Kumukahi, Hawaii, than the standard case prediction.

The substitution of an industrial CO<sub>2</sub> source having a southward shift in emissions compared with the standard case produces a slightly better fit (4.11). The shifts in emissions

are substantial, but the inferred terrestrial biospheric fluxes are altered to a similar extent so that the chi-square criterion is not a sensitive approach to deciding the distribution of these emissions. This is not surprising since the model cannot distinguish terrestrial biospheric CO<sub>2</sub> from industrial CO<sub>2</sub>.

Chi-square for all other tests departs only moderately from that for the standard case, providing only limited guidance as to whether alternatives are likely to be more realistic than the standard case. Moving tropical biospheric boundaries to 16° (3.87) or adding an oceanic boundary at 47°S. (4.02) modestly improves the fit, while adding a similar oceanic boundary in the northern hemisphere (4.32), shifting the northern temperate biospheric boundary to 55°N. (4.33), or interposing zero buffer zones between the biospheric zones (4.14) have almost no effect.

### 8.3 Comparison of long-term average inferred fluxes with the standard case

With a few exceptions, the fluxes simulated in the sensitivity tests depart only minimally from the standard case with respect to their average values. Changes resulting from relocating the boundary between the northern temperate and boreal zones (see Figure 9) result in substantial shifts in fluxes only because they are compared at the boundary of the standard case. Changes in the spatial distribution of industrial CO<sub>2</sub> emissions (see Figure 20) understandably cause fluxes to change in almost direct proportion. Neglecting temperature-dependent isotopic fractionation causes a large decrease in the tropical biospheric flux (see Figure 25), but this case is readily rejected because of its high chi-square value and violation of a known phenomenon. There are significant changes in flux over almost all zones when different wind data are used (see Figures 1 and 4) by as much as 0.9 PgC yr<sup>-1</sup>. These differences, indeed, may not indicate the full range of discrepancy that incorrect specification of winds may produce, because we have no test of the use of both wind and convection data for the record period as a whole.

A single critical case of a large shift in average fluxes from the standard case that cannot be ruled out by the chi-square criterion, or attributed to a well identified cause, is our preferred case in which the terrestrial fluxes for the grid box of La Jolla are removed (see subsection 5.3, above) to compensate for the use of model predictions of atmospheric CO<sub>2</sub> for all days of the year, whereas the observations with which the model compares are only for times of onshore winds.

### 8.4 Preferred case

The magnitudes of the zonal net terrestrial biospheric fluxes inferred in the standard case, discussed above, are surprisingly large compared with our estimates of the net primary production of terrestrial vegetation (NPP) for the same zones (Table 3). The northern temperate flux is especially large: 33% of NPP estimated from satellite data (Article I, Table 5) averaged over the 1990's. The only sensitivity tests that seriously dispute this large flux involve the removal of the terrestrial fluxes from near La Jolla (Figure 15), removal from just the La Jolla grid

box resulting in the smallest flux. We cannot demonstrate that any of these cases infer more nearly correct fluxes than for the standard case, but we propose to adopt the first mentioned case (Figure 15a) as a "preferred case" because the temperate zone flux is reduced to a probably more reasonable 18% of NPP for the 1990's and because removal over a larger area (Figure 15b) reverses the effect on the temperate flux. The other biospheric fluxes averaged over the 1990's are also reduced in this preferred case, the northern polar, reduced from 9% of NPP to near zero, and the tropical from 10% to 8%. The small flux for the southern temperate zone is hardly changed. (The negligible flux for 47°-90°S is shown in Table 3 only to produce consistent global totals controlled by the double deconvolution calculations of Article I).

### 8.5 Decadal variability

The atmospheric CO<sub>2</sub> records of this study are long enough to discern variability on the decadal time-scale, although shorter-term variability makes uncertain whether these decadal trends are significant. Obviously variable is the release of fossil fuel CO<sub>2</sub> that, on the basis of direct information on fuel consumption, increased from about 5 PgC yr<sup>-1</sup> at the beginning of the record to about 7 PgC yr<sup>-1</sup> at the end. Over this time interval, the global average oceanic flux almost surely became more of a sink, and the sink tendency of the global average terrestrial biospheric flux probably increased as well (see Article I, Figure 10, and Table 7), in response to the growing industrial CO<sub>2</sub> source.

These decadal trends are reflected in the regional fluxes of this study, but are not the only cause of regional decadal variability. Although the temperate fluxes in both hemispheres, following the global trend, became stronger sinks in the 1990's, the tropical flux became more of a source, suggestive of either a human caused change in land use or a climatic change. The sensitivity tests produce only small changes in decadal trends compared with the standard case, except trivially when the northern boundary of the northern temperate biospheric source component is moved northward (Figure 9). There are also decadal changes in fluxes when station records are removed from the inversion calculations (Figures 13 and 14). These changes are seen to be artifacts of the variable number of stations contributing data to the calculations in the standard case.

Removing the terrestrial fluxes for the grid box of La Jolla, and also moving the location of this station away from the coastline (Figure 16), causes changes in the decadal trend of the biospheric flux in the northern temperate zone from the standard case related to the progressively greater importance of fossil fuel CO<sub>2</sub> as a nearby contributor to the fluxes. Finally, any errors in specifying regional trends in CO<sub>2</sub> emissions from combustion, as illustrated by an example where emissions are shifted southward relative to the standard case (Figure 21) are almost directly transmitted into changes in trends of the terrestrial biospheric fluxes. Thus the sensitivity tests do not significantly challenge the decadal variability found in the standard case, provided that the fossil fuel data of that case are correct.

### 8.6 Short-term interannual variability

Shorter term variability in fluxes, reflecting variability in atmospheric CO<sub>2</sub> concentration and in <sup>13</sup>C/<sup>12</sup>C ratio, correlates strongly with El Niño events. All stations show similar variability because the interval between events, shown by gray bars in the plots of regional fluxes in this article, is long compared with the time for the earth's atmosphere to mix globally, approximately one year. Conversely, the inferred fluxes for the temperate zones and boreal zone show little relation to the times of El Niño events. No sensitivity test challenges this finding of a mainly tropical El Niño variability of biospheric flux.

A likely source of error, not addressed here by any sensitivity test, is the neglect to attribute some of the variability in <sup>13</sup>C/<sup>12</sup>C ratio to temporal variability in the carbon isotopic fractionation ("discrimination") attending photosynthesis of land plants. Because of the close phase relation of short-term interannual fluctuations in both CO<sub>2</sub> concentration and <sup>13</sup>C/<sup>12</sup>C ratio with El Niño events (clearly seen in Article I, Figure 7), variable discrimination is likely to explain the fluctuations that our calculations infer for tropical fluxes only to the extent that discrimination has varied in phase with tropical NPP. But a covariation of discrimination with NPP is likely, driven by variable stress to tropical plants (Article 1, subsection 7.4). Even by neglecting variability in discrimination of tropical vegetation by as little as 1‰, from one El Niño event to the next (see Article I, subsection 5.2), the amplitude of fluctuation in tropical biospheric flux would be reduced by about 2 PgC yr<sup>-1</sup>, cancelling out approximately a third of the inferred amplitude associated with the major El Niño events of 1983, 1987, and 1998, and much of the variability of the tropical oceanic flux related to these events.

Of the sensitivity tests that produce reasonable fits to the atmospheric data, as indicated by reduced chi-square values, few show any significant alteration in the patterns of short-term interannual variability from the standard case. Most notable is a decrease in variability of about 25% for the boreal zone, when interannually-varying winds are used in place of winds only for 1986 in the standard case (Figure 4). Still more short-term variability, and perhaps some longer term variability, would probably correlate with transport in our calculations if interannually variable vertical convection fields were incorporated, a subject for future studies. That convection as well as winds is likely to be important is seen in a sensitivity test (Figure 5) where the atmospheric tracer transport model, TM2, of the standard case is replaced with TM3 having quite different vertical convection fields, causing the simulated tropical biospheric fluxes to be stronger sources, the boreal and southern temperate to be weaker.

Most remarkable is that withdrawing the use of <sup>13</sup>C/<sup>12</sup>C data as a control on interannual variability (Figure 17), although it causes marked reductions in fluctuations of the tropical biospheric flux and represses variability of the southern temperate biospheric flux, causes only small changes in the interannual patterns of the simulated biospheric fluxes of the northern temperate and boreal zones. We thus conclude that the interannual variability computed in the standard case

simulations, except in relation to wind and vertical convection, and possibly to variations in isotopic discrimination by plants, arises mainly from variability in the atmospheric CO<sub>2</sub> input data, not from characteristics of the inversion model.

#### ADDENDUM

We have not updated to 1999 a substantial fraction of the sensitivity tests computed only through 1998. Our findings are not likely to change by adding one more year of model simulations. However, Table 2, for uniformity, shows averages of chi-square in the 1990's just for 1990-1998.

#### ACKNOWLEDGMENT

We are grateful to M. Heimann of the Max Planck Institute for Biogeochemistry, Jena, Germany for helpful discussions, and for supplying transport model code, wind fields, and calculations. We are grateful to T. Boden, G. Marland, and A. Brenkert of Oak Ridge National Laboratory, Tennessee and R. Andres of the University of Alaska, Fairbanks, for assistance with identifying alternative sources of industrial emissions. Funding for this research was provided by the U.S. National Aeronautics and Space Administration, U.S. National Science Foundation, and U.S. Department of Energy by grants NASA NAG5-3469, NSF ATM 97-11882, NSF OCE 97-25995, and DOE DE-FG03-95ER62075, and by the Office of the Director of the Scripps Institution of Oceanography.

#### REFERENCES

- [1] Andres, R. J., G. Marland, T. Boden, and S. Bischof, Carbon dioxide emissions from fossil fuel consumption and cement manufacture, 1751-1991 and an estimate of their isotopic composition and latitudinal distribution, in *The Carbon Cycle*, edited by T. M. L. Wigley and D. S. Schimel, pp. 53-62, Cambridge University Press, Cambridge, 2000.
- [2] Bolin, B., and C. D. Keeling, Large-scale atmospheric mixing as deduced from the seasonal and meridional variations of carbon dioxide, *Journal of Geophysical Research*, *68*, p. 3899-3920, 1963.
- [3] Brenkert, A. L., Marland, G., T. A. Boden, R. J. Andres, and J. G. J. Olivier, Carbon Dioxide Emission Estimates from Fossil-Fuel Burning, Hydraulic Cement Production, and Gas Flaring for 1995 on a One Degree Grid Cell Basis (NDP-058A) ORNL/CDIAC, NDP058a, Carbon Dioxide Analysis Center, Oak Ridge, Tenn., 1998.
- [4] Ciais, P., P. P. Tans, J. W. C. White, M. Trolier, R. J. Francey, J. A. Berry, D. R. Randall, P. J. Sellers, J. G. Collatz, and D. S. Schimel, Partitioning of ocean and land uptake of CO<sub>2</sub> as inferred by  $\delta^{13}\text{C}$  measurements from the NOAA Climate Monitoring and Diagnostics Laboratory Global Air Sampling Network, *Journal of Geophysical Research - Atmospheres*, *100(D3)*, 5051-5070, 1995.
- [5] Denning, A. S., I. Y. Fung, and D. Randall, Latitudinal gradient of atmospheric CO<sub>2</sub> due to seasonal exchange with land biota, *Nature*, *376*, 240-243, 1995.
- [6] Denning, A. S., M. Holzer, K. R. Gurney, M. Heimann, R. M. Law, P. J. Rayner, I. Y. Fung, S.-M. Fan, S. Taguchi, P. Friedlingstein, Y. Balkanski, J. Taylor, M. Maiss, and I. Levin, Three-dimensional transport and concentration of SF<sub>6</sub>. A model intercomparison study (TransCom 2), *Tellus 51B*, 266-297, 1999.
- [7] ECMWF (European Center for Medium-Range Weather Forecasts), Evolution of the ECMWF analysis and forecasting system, Part II, pages 9-20, in November, 1999 technical supplement to the The Description of the ECMWF/WCRP Level III-A Global Atmospheric Data Archive, ECMWF Operations Department, Shinfield Park, Reading, Berkshire RGE 9AX, England, 1999.
- [8] Gibson, J.K., P. Kallberg, S. Uppala, A. Nomura, and E. Serrano, ERA description, *ECMWF Reanal. Proj. Rep. Ser.*, *1*, 72 pp., Eur. Cent. for Medium-Range Weather Forecasts, Reading, England, 1997.
- [9] Heimann, M., The global atmospheric tracer model TM2, *Deutsches Klimarechenzentrum Technical Report No. 10*, 53 pp., Hamburg, Germany, 1995.
- [10] Heimann, M., C. D. Keeling, and C. J. Tucker, A three-dimensional model of atmospheric CO<sub>2</sub> transport based on observed winds: 3. Seasonal cycle and synoptic time scale variations, in *Aspects of Climate Variability in the Pacific and the Western Americas*, *Geophysical Monograph*, vol. 55, Edited by D. H. Peterson, pp. 277-303, AGU, Washington, D.C., 1989.
- [11] Heimann, M., and C. D. Keeling, A three-dimensional model of atmospheric CO<sub>2</sub> transport based on observed winds: 2. Model description and simulated tracer experiments, in *Aspects of Climate Variability in the Pacific and the Western Americas*, *Geophysical Monograph*, vol. 55, Edited by D. H. Peterson, pp. 237-275, AGU, Washington, D.C., 1989.
- [12] Hunt, E. R., S. C. Piper, R. Nemani, C. D. Keeling, R. D. Otto, and S. W. Running, Global net carbon exchange and intra-annual atmospheric CO<sub>2</sub> concentrations predicted by an ecosystem process model and three-dimensional atmospheric transport model, *Global Biogeochemical Cycles*, *10*, 431-456, 1996.
- [13] Jacob, D. J., M. J. Prather, S. C. Wofsy, and M. B. McElroy, Atmospheric distribution of <sup>85</sup>Kr simulated with a general circulation model, *Journal of Geophysical Research*, *92*, 6614-6626, 1987.
- [14] Keeling, C. D., Harris, T. B., and Wilkins, E. M., Concentration of atmospheric carbon dioxide at 500 and 700 millibars, *Journal of Geophysical Research*, *3*, 4511-4528, 1968.
- [15] Keeling, C. D., S. C. Piper, and M. Heimann, A three-dimensional model of atmospheric CO<sub>2</sub> transport based on observed winds: 4. Mean annual gradients and interannual variations, in *Aspects of Climate Variability in the Pacific and the Western Americas*, *Geophysical Monograph*, vol. 55, edited by D. H. Peterson, pp. 305-363, AGU, Washington, D. C., 1989.
- [16] Keeling, C. D., T. P. Whorf, M. Wahlen, and J. van der Plicht, Interannual extremes in the rate of rise of atmospheric carbon dioxide since 1980, *Nature*, *375*, 666-670, 1995.
- [17] Keeling, C. D., J. F. S. Chin, and T. P. Whorf, Increased activity of northern vegetation inferred from atmospheric CO<sub>2</sub> measurements, *Nature*, *382*, 146-149, 1996.
- [18] Keeling, C. D., S. C. Piper, R. B. Bacastow, M. Wahlen, T. P. Whorf, M. Heimann, and H. A. Meijer, Exchanges of atmospheric CO<sub>2</sub> and <sup>13</sup>CO<sub>2</sub> with the terrestrial biosphere and oceans from 1978 to 2000. I. Global aspects, SIO Reference Series, No. 01-06 (Revised from SIO Reference Series, No. 00-21), Scripps Institution of Oceanography, San Diego, 2001.
- [19] Keeling, C. D., and S. C. Piper, Exchanges of atmospheric CO<sub>2</sub> and <sup>13</sup>CO<sub>2</sub> with the terrestrial biosphere and oceans from 1978 to 2000. IV. Critical overview, SIO Reference Series, No. 01-09 (Revised from SIO Reference Series, No. 00-24), Scripps Institution of Oceanography, San Diego, 2001.
- [20] Lancaster, J., Carbon dioxide variations: ocean air sampling near Hawaii and Southern California from July 1983 to September 1984, Master's Thesis, University of California, San Diego, 179 pp., 1985.
- [21] Li, Y.-F., Global Population Distribution (1990), Terrestrial Area and Country Name Information on a One by One Degree Grid Cell Basis, ORNL/CDIAC-96, DB1016, Carbon Dioxide Analysis Center, Oak Ridge, Tenn., <http://cdiac.esd.ornl.gov/ndps/db1016.html>, 1996.
- [22] Piper, S. C., C. D. Keeling, M. Heimann, and E. F. Stewart, Exchanges of atmospheric CO<sub>2</sub> and <sup>13</sup>CO<sub>2</sub> with the terrestrial biosphere and oceans from 1978 to 2000. II. A three-dimensional tracer inversion model to deduce regional fluxes, SIO Reference Series, No. 01-07 (Revised from SIO Reference Series, No. 00-22), Scripps Institution of Oceanography, San Diego, 2001a.
- [23] Piper, S. C., C. D. Keeling, and E. F. Stewart, Exchanges of atmospheric CO<sub>2</sub> and <sup>13</sup>CO<sub>2</sub> with the terrestrial biosphere and oceans from 1978 to 2000. III. Sensitivity tests, SIO Reference Series, No. 01-08 (Revised from SIO Reference Series, No. 00-23), Scripps Institution of Oceanography, San Diego, 2001b.